Hyperboloidal slicing approach to quasi-normal mode expansions: the Reissner-Nordström case

Rodrigo Panosso Macedo,[1] José Luis Jaramillo,[2] and Marcus Ansorg[3]

[1]*School of Mathematical Sciences, Queen Mary, University of London,*
Mile End Road, London E1 4NS, United Kingdom
[2]*Institut de Mathématiques de Bourgogne (IMB), UMR 5584, CNRS,*
Université de Bourgogne Franche-Comté, F-21000 Dijon, France
[3]*Theoretisch-Physikalisches Institut, Friedrich-Schiller-Universität Jena,*
Max-Wien-Platz 1, D-07743 Jena, Germany
(Dated: March 25, 2019)

We study quasi-normal modes of black holes, with a focus on resonant (or quasi-normal mode) expansions, in a geometric frame based on the use of conformal compactifications together with hyperboloidal foliations of spacetime. Specifically, this work extends the previous study of Schwarzschild in this geometric approach to spherically symmetric asymptotically flat black hole spacetimes, in particular Reissner-Nordström. The discussion involves, first, the non-trivial technical developments needed to address the choice of appropriate hyperboloidal slices in the extended setting as well as the generalization of the algorithm determining the coefficients in the expansion of the solution in terms of the quasi-normal modes. In a second stage, we discuss how the adopted framework provides a geometric insight into the origin of regularization factors needed in Leaver's Cauchy based foliations, as well as into the discussion of quasi-normal modes in the extremal black hole limit.

I. INTRODUCTION

Black-hole perturbation theory represents one of the cornerstones in the development of General Relativity. Initially developed in the context of astrophysical problems, its applications nowadays are spread among many areas in gravitational physics. Focusing on the decaying properties of propagating fields, the time evolution of perturbative fields on a background containing a black hole presents (after an initial transitory) a characteristic behavior at intermediate time scales: a decay in terms of a discrete set of exponentially damped oscillations, the so-called quasi-normal modes (QNMs). Most importantly, the decay and oscillation time scales are signatures of the background spacetime. QNMs have found a wide range of application in the settings of gravitational wave detection, mathematical relativity, the gauge/gravity duality, string theory, brane-world models and quantum gravity — see e.g. [1] for a classical reference and [2–5] for a revision along the past few decades. For spacetimes whose curvature (more precisely the effective potential in the appropriate wave equation) does not decay sufficiently fast at large distances, e.g. Schwarzschild, one identifies a second behavior in the final stages the evolution. For late times, a power law decay — the so-called tail decay — may dictate the dynamics [6, 7].

In fact, the exponentially damped oscillatory decay is not a feature exclusive to linear fields propagating on black-hole spacetimes, but rather a generic behavior of solutions in open dissipative systems described by wave equations subject to outgoing boundary conditions. Such concept of QNM is essentially related to the notion of resonance in scattering theory and has acquired, in recent years, a major role in other domains. In particular, it is remarkable the synergy with recent developments in the optical study of nano-resonators (cf. [8]) as well as in the mathematical literature, where they are usually referred to as 'scattering resonances' [9, 10].

When considering closed (compact) conservative systems, with dynamics characterized in terms of self-adjoint operators, the notion of normal mode provides a powerful tool to analyze the system, in particular by making use of the completeness of normal eigenfunctions $\psi_n(x^k)$ to expand the solutions $\Psi(t, x^k)$

$$\Psi(t, x^k) = \sum_{n=0}^{\infty} \eta_n \psi_n(x^k) e^{i\omega_n t} , \qquad (1)$$

where the amplitudes coefficients η_n are obtained from the projection of the initial data onto the complete orthonormal system of eigenfunctions by using the scalar inner product (this is guaranteed by the so-called 'spectral theorem' associated with self-adjoint operators). In certain respects, QNMs represent in open systems the counterpart to normal modes in closed systems. In this sense, it is natural to pose the question about the possibility of writing an expression of the type (1) for solutions of initial value problems associated with linear dissipative wave equations in terms of QNM expansions. More precisely, it is natural to try to assess the existence of appropriate space and time scales for which such dissipative solutions admit well-defined approximations in terms of QNM expansions.

However, in such dissipative scenarios, the relevant differential operator associated with the wave equation is no longer self-adjoint. In particular, this amounts to a loss of a corresponding spectral theorem, so that QNMs do not generically constitute a complete set. Moreover, orthogonality is also generically lost, so that even if completeness is preserved, the straightforward projection algorithm to determine the coefficients is no longer available.

On the other hand, in the context of stationary black-hole spacetimes, the time coordinate t usually employed to parametrize the dynamical evolution of the fields actually foliates the spacetime into time-constant surfaces extending between the bifurcation sphere $\mathcal{B}$ and spatial infinity i^0. Within

the setting of such Cauchy foliations, the dissipative character comes about only after one introduces the correct outgoing boundary conditions in the spatial asymptotic regions. As a consequence, the eigenfunctions $\psi_n(x^k)$ present an undesirable exponentially growth near the boundaries. This property constitutes one of the main drawbacks in the understanding of the technical and conceptual issues involved in such attempted 'resonant expansion' representations of the form (1).

Indeed, in a recent article [11], black-hole perturbation theory on the Schwarzschild background was revisited within the geometrical framework provided by a spacetime foliation in terms of horizon-penetrating hyperboloidal slices (cf. [12] for a previous discussion of these ideas in the specific setting of quasinormal modes, as well as [13, 14] for seminal work along these lines). The authors argue and demonstrate numerically that if the initial data are analytical in terms of a compactified coordinate in the appropriate hyperboloidal slices, a superposition of the form

$$\Phi(\tau, x^k) = \sum_{n=0}^{\infty} \eta_n \phi_n(x^k) e^{s_n \tau} + \int_{-\infty}^{0} \eta(s)\phi(x^k; s)e^{s\tau}ds \,,$$
(2)

can be constructed for solutions corresponding to initial value problems of linear wave equations in the Schwarzschild spacetime.

Note that the spectral decomposition (2) includes not only the (discrete) QNM expansion, but also a contribution from the continuous spectrum along the negative real line $\Re(s) < 0$. This term, responsible for the late-time tail decay, results from the existence of a branch cut along $\Re(s) < 0$ in the analytical extension of the corresponding propagator operator [1].

More specifically, a semi-analytical algorithm was developed allowing to calculate all the elements of the spectral decomposition (2), i.e., the QNMs s_n together with the functions $\phi_n(x^k)$ and $\phi(x^k; s)$ (depending only on the structure of the wave equation) as well as the amplitudes η_n and $\eta(s)$ (read from the initial data). The study in [11] led to the following conjecture [2]:

Conjecture 1. *Given analytical initial data Φ_0 and $\dot{\Phi}_0$ for the wave equation, the spectral decomposition (2) holds for all $\tau > \nu$ where ν is the mutual growth rate of $|\eta_n \phi_n|$ and $|\eta(s)\phi(s)|$, i.e., the QNM and branch cut excitation coefficients.*

---

[1] Given the elliptic operator $P_V = -\Delta + V(x)$ obtained from the wave equation upon a Laplace transform, QNMs are associated with the poles in the 'analytical extension' of the Green's function corresponding to $(P_V + s^2)$ into the whole complex s-plane (see appendix VII A for a discussion in a spectral setting). For effective potentials $V(x)$ not decaying sufficiently fast at infinity — for instance in the Schwarzschild case — a branch cut starting at $s = 0$ appears in addition to the QNM first-order poles.

[2] The symbol $\sum_{n=0}^{\infty}$ in expression (2) must be understood in a formal sense. More precisely, the semi-analytical algorithm in [11] does not allow to fully settle the convergence properties of the series in (2). Specifically, we do not claim here QNM (extended with tails) completeness: conjecture 1 must be understood rather in terms of an 'asymptotic expansion'. See appendix VII A.

Even though the generic ideas introduced in [11] are aimed at a broader context, the semi-analytical algorithm developed there is tailored for the Schwarzschild spacetime. Nevertheless, the well-defined time-scale ν introduced in conjecture 1 is used in the context of the AdS/CFT correspondence [15] (yet, some technical calculations had to be addressed by a different method).

In this paper, we extend the formulation of the spectral decomposition (2) in the framework of hyperboloidal slices for fields propagating on a spherically symmetric, not necessarily vacuum, asymptotically flat spacetime. Despite the restriction to spherically symmetric solutions, such first step generalization already displays several features that enlighten the theoretical discussion and introduces technical challenges for the algorithm used in the calculation of all the elements within the spectral decomposition (2). Specifically, our main focus lies on the Reissner-Nordström case. Yet, one could envisage further scenarios — for instance, solutions describing a central black hole and a surrounding shell composed out of collision-less Einstein-Vlasov-matter [16] or, relaxing the conditions on dimensionality and asymptotic structure, higher-dimensional spacetimes [17, 18] and asymptotically AdS spacetimes [19, 20] — for which the technicalities of the methods presented here could be appropriately adapted.

In the first part, this article is framed in the study of the geometrical aspects of the formalism as well as in the technical generalization of the semi-analytical algorithm developed in [11] for the calculation of all elements in (2). In particular, while reviewing the construction of the spatially compactified hyperboloidal slices in a generic context, we explicitly identify in section II the gauge degrees of freedom associated with the hyperboloidal foliation and the conformal compactification. This allows us to introduce a gauge optimally adapted to the study of black-hole perturbation theory within the present hyperboloidal framework, which we refer to as the *minimal gauge*. Then, we discuss in section III the formal aspects for the construction of the desired spectral decomposition (2). For this task, we first identify the correct conformally invariant wave equation to be solved. Next, a Laplace transform is applied to the wave equation in question and a spatial differential equation arises with an inhomogeneity determined by the initial data. This system is parametrized by the complex Laplace parameter s. The spectral decomposition (2) is then obtained by the deformation of the inverse Laplace path integration which collects the contribution coming from the operator's poles and branch cut in the complex $s-$plane. Finally, section IV describes in detail the generalized algorithm in the frequency domain to calculate the various ingredients of the spectral representation (2). The algorithm is based on the expansion of the relevant functions into a Taylor series. Thus, the corresponding spatial differential equation gives rise to a recurrence relation determining the coefficients of the Taylor expansion. While in [11], the algorithm was restricted to a 3-term recurrence relation, we generalize it here into an arbitrary (but finite) $(m + 2)$-terms recurrence relation.

In a second stage, we discuss extensively the application of the formalism to the particular case of the Reissner-Nordström solution. In particular, we show in section V that the min-

imal gauge leads naturally to two choices for the conformal representations of the spacetime. It turns out that the two geometries have different spacetime limits in the extremal case [21, 22]. When approaching extremality, one gauge leads to the usual extremal Reissner-Nordström black hole [23] whilst the second one shows a discontinuous transition to the near-horizon geometry [24, 25] (see [26] for a review on near-horizon geometries) described by the Bertotti-Robinson metric [27, 28]. Interestingly, we actually observe that the gauge leading to the Bertotti-Robinson spacetime represents the precise counterpart, in the present geometrical framework, to the treatment introduced by Leaver [29]. Indeed, the geometrical approach based on conformally compactified spacetimes foliated by hyperboloidal slices straightforwardly recovers all factors introduced in [29] accounting for the correct boundary conditions leading to the QNMs.

We work with units such that the speed of light as well as Newton's constant of gravity are unity, $c = G = 1$.

II. THE GEOMETRICAL FRAMEWORK

We begin by reviewing the construction of hyperboloidal slices in a spherically symmetric black-hole spacetime and by introducing a gauge which is best adapted to the present discussion of black-hole perturbation theory.

A. Schwarzschild coordinates

We start with a stationary (actually static) spherically symmetric line element in the form given by Schwarzschild coordinates $\{t, r, \theta, \varphi\}$

$$ds^2 = -f(r)\,dt^2 + f(r)^{-1}\,dr^2 + r^2\,d\omega^2 \,, \qquad (3)$$

with $d\omega^2 = d\theta^2 + \sin(\theta)^2\,d\varphi^2$ the metric of the unit $2-$sphere. We assume that the function $f(r)$ satisfies the following conditions:

(i) Asymptotic flatness expansion:

$$f(r) \sim 1 - \frac{2M}{r} + o\left(\frac{1}{r}\right) \,; \qquad (4)$$

(ii) Killing (black-hole) horizon at $r_\mathcal{H}$:

$$f(r_\mathcal{H}) = 0 \,; \qquad (5)$$

(iii) $f(r)$ is a polynomial in $1/r$.

While assumptions (i)-(ii) are natural for an asymptotically flat black-hole spacetime, the assumption (iii) is motivated by the form of well-known spherically symmetric exact solutions. The tortoise coordinate $r^* = r^*(r)$ is fixed (up to a constant) by

$$\frac{dr^*}{dr} = \frac{1}{f(r)} \,. \qquad (6)$$

Along the slices of constant coordinate time t, the horizon surface $r = r_\mathcal{H}$ ($r^* \to -\infty$) corresponds to the bifurcation sphere $\mathcal{B}$, while $r \to +\infty$ ($r^* \to +\infty$) corresponds to spatial infinity — see Fig. 1.

B. Ingoing Eddington-Finkelstein coordinates

While in [12, 30] the hyperboloidal coordinates follow directly from the coordinates $\{t, r, \theta, \varphi\}$, here we first consider an intermediate step that enforces horizon-penetrating slices via the ingoing Eddington-Finkelstein coordinates. Besides, we can already at this stage discuss the compactification of the spacetime.

Spatially compactified and dimensionless ingoing Eddington-Finkelstein coordinates $\{\bar{v}, \sigma, \theta, \varphi\}$ are given by

$$r = \lambda\frac{\rho(\sigma)}{\sigma}, \quad t = \lambda\bar{v} - r^*(r(\sigma)) \,, \qquad (7)$$

with λ a length scale of the spacetime, typically related here to the event horizon radius $r_\mathcal{H}$. The line element reads

$$ds^2 = \frac{\lambda^2}{\sigma^2}\left[-\sigma^2 F\,d\bar{v}^2 - 2\beta\,d\bar{v}\,d\sigma + \rho^2\,d\omega^2\right] \,, \qquad (8)$$

with ρ, F and β functions of the coordinate σ. In particular, $F(\sigma) = f(r(\sigma))$ is the metric function, while

$$\beta(\sigma) = \rho(\sigma) - \sigma\rho'(\sigma) \,, \qquad (9)$$

is the radial component of the shift and therefore corresponds to a gauge freedom in the choice of the coordinate σ — see discussion in section II C 2.

Finally, $\rho(\sigma)$ is the areal radius in the conformal representation of the spherically symmetric spacetime, whose conformal metric is given by

$$d\tilde{s}^2 = \Omega^2 ds^2, \quad \Omega = \frac{\sigma}{\lambda} \,. \qquad (10)$$

As such, we impose ρ to be a regular function on its domain attaining positive values (in particular, non-vanishing). Moreover, we assume $\rho(\sigma)$ to be such that $\beta(\sigma) > 0$ — see Eq.(9).

The outgoing and ingoing null vectors in the conformal spacetime (normalized as $\tilde{g}_{ab}\tilde{l}^a\tilde{k}^b = -1$) are given, respectively, by

$$\tilde{l}^a = \zeta^{-1}\left[\delta^a_{\bar{v}} - \frac{\sigma^2 F}{2\beta}\delta^a_\sigma\right], \quad \tilde{k}^a = \frac{\zeta}{\beta}\delta^a_\sigma \,. \qquad (11)$$

The free boost-parameter ζ will be fixed in the next section.

C. Hyperboloidal coordinates

We finally introduce the hyperboloidal coordinates $\{\tau, \sigma, \theta, \varphi\}$ via the height technique [30]

$$\tau = \bar{v} + h(\sigma) \,. \qquad (12)$$

In the new coordinates, the conformal line element is

$$d\tilde{s}^2 = -\sigma^2 F d\tau^2 + h' \left[2\beta - \sigma^2 F h'\right] d\sigma^2$$
$$- 2 \left[\beta - \sigma^2 F h'\right] d\tau d\sigma + \rho^2 d\omega^2 . \quad (13)$$

The height function $h(\sigma)$ must be specified in such a way that the spacelike hypersurfaces $\tau = $ constant foliate future null infinity. This property is guaranteed by requiring τ to be a good parameter of the (future) ingoing null vector, that is

$$\tilde{k}^a \partial_a \tau = 1 . \quad (14)$$

1. The height function

In the coordinates $\{\tau, \sigma, \theta, \varphi\}$, the components of the ingoing/outgoing null vectors are respectively

$$\tilde{k}^a = \delta_\tau^a + \frac{1}{h'}\delta_\sigma^a , \quad (15)$$

$$\tilde{l}^a = \frac{h'}{2\beta^2} \left(2\beta - \sigma^2 F h'\right) \delta_\tau^a - \frac{\sigma^2 F}{2\beta^2} h' \delta_\sigma^a . \quad (16)$$

Consistently with (14), the boost parameter ζ present in (11) has been fixed here such that $\tilde{k}^\tau = 1$. Then, the condition

$$\lim_{\sigma \to 0} \tilde{k}^a = \delta_\tau^a \Rightarrow \lim_{\sigma \to 0} \frac{1}{h'} = 0 , \quad (17)$$

guarantees that $\sigma = 0$ (along $\tau = \text{const.}$) is a null surface, corresponding actually to *future* null infinity (as opposed to the *past* character of $\sigma = 0$, along $\bar{v} = \text{const.}$, arising in ingoing Eddington-Finkelstein coordinates [3] is section II B).

Besides, we want to ensure that the components of the vector $\tilde{l}^a$ remain finite as $1/h' \to 0$. Let us first assume the generic expansion

$$\beta(\sigma) = \beta_0 + \beta_1 \sigma + \mathcal{O}(\sigma^2) . \quad (18)$$

The presence of the term β_1 in this expansion is, however, undesirable. Indeed, according to its definition (9), the areal radius $\rho(\sigma)$ assumes the form

$$\rho(\sigma) = \beta_0 + \beta_1 \sigma - \beta_1 \sigma \ln \sigma + \mathcal{O}(\sigma^2) . \quad (19)$$

Thus, the condition $\beta_1 = 0$ is required for eliminating the logarithmic singularity at $\sigma = 0$. It is also convenient to identify $\beta_0 = \rho_0$.

Then, we recall the assumption (i) for the function $f(r)$ which, together with Eq. (7), gives rise to the expansion

$$F(\sigma) = 1 - \frac{2M}{\lambda \rho_0} \sigma + \mathcal{O}(\sigma^2) . \quad (20)$$

---

[3] The transformation from ingoing Eddington-Finkelstein $\{\bar{v}, \sigma, \theta, \phi\}$ to hyperboloidal coordinates $\{\tau, \sigma, \theta, \phi\}$ is a coordinate change in the conformal spacetime involving only the "time" coordinate. Static observers parametrized by $\sigma = $ const. are not affected by it. The limiting procedure $\sigma \to 0$ is taken along $\bar{v} = $ const. if treated in ingoing Eddington-Finkelstein or along $\tau = $ const. if performed in hyperboloidal coordinates. The former leads to past null infinity $\mathscr{I}^-$ whereas the latter to future null infinity $\mathscr{I}^+$, both geometrically defined asymptotic notions — see Fig. 1.

As $\sigma \to 0$, a finite value for the component $\tilde{l}^\tau$ is obtained for

$$h'(\sigma) = \frac{2\rho_0}{\sigma^2} \left[1 + \frac{2M}{\rho_0 \lambda}\sigma\right] + \mathcal{O}(1) . \quad (21)$$

This result ensures the regularity of $\tilde{l}^\sigma$ as well. Integrating Eq. (21) leads to

$$h(\sigma) = -2\rho_0 \left[\frac{1}{\sigma} - \frac{2M}{\lambda \rho_0} \ln \sigma\right] + A(\sigma) . \quad (22)$$

The regular free function $A(\sigma)$ represents a freedom in the choice of the hyperboloidal foliation, to be fixed in the next section.

Finally, the condition $\tilde{\nabla}_a \tau \tilde{\nabla}^a \tau < 0$ (for having spacelike surfaces $\tau = $ constant) imposes

$$0 < \sigma^2 h' < \frac{2\beta}{F} . \quad (23)$$

2. The minimal gauge

In the previous sections, $\beta(\sigma)$ and $A(\sigma)$ were identified as gauge degrees of freedom. The former related to the definition of the compact coordinate σ — and thus to the choice of the conformal representation of the spacetime (10) — while the latter distinguishes different hyperboloidal foliations.

Given the freedom in β, we choose it to be constant, this leading to a gauge where

$$\beta(\sigma) = \rho_0 \Rightarrow \rho(\sigma) = \rho_0 + \rho_1 \sigma . \quad (24)$$

In terms of the coordinate σ, it is very convenient to fix the event horizon to the value $\sigma_{\mathcal{H}} = 1$. This particular choice constraints the relation between ρ_0 and ρ_1 to

$$\rho_0 = \frac{r_{\mathcal{H}}}{\lambda} - \rho_1 . \quad (25)$$

The freedom provided by $A(\sigma)$ can be used to specify further geometrical properties of the hyperboloidal slices, such as a constant mean curvature [30–33]. By allowing an angular dependence in the function A, one can even depart from spherical symmetry [34, 35] in the coordinate description. We restrict ourselves to the simplest case

$$A(\sigma) = 0 . \quad (26)$$

We refer to the choices (24) and (26) as the *minimal gauge*. Indeed, the degrees of freedom from the radial compactification and from the hyperboloidal foliation are reduced to a minimum and they consist merely in fixing the scaling parameter λ and the value ρ_1. All relevant quantities in the line element (13) are determined essentially by the properties of the function $F(\sigma)$. In particular, recalling assumption (iii), all components of the metric tensor become polynomials in σ.
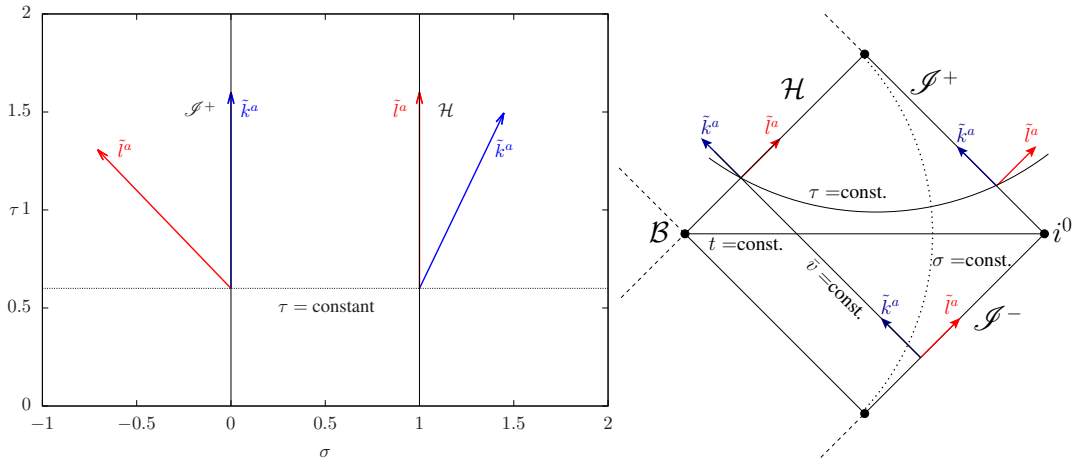
FIG. 1. Left panel: conformal null vectors in the spatially compactified spacetime with metric $\tilde{g}_{ab}$ in terms of the hyperboloidal coordinates $\{\tau, \sigma\}$. At $\sigma = 0$ and $\sigma = 1$ the light-cones point outwards the domain $\sigma \in [0, 1]$. Such surfaces corresponds, respectively, to future null infinity and the black-hole horizon. Right panel: Carter-Penrose conformal diagram for the external region of an asymptotically flat, stationary black-hole spacetime. The time-constant surface in the (initial) Schwarzschild coordinates $\{t, r\}$ extends between the bifurcation sphere $\mathcal{B}$ ($r = r_{\mathcal{H}}$) and spatial infinity i^0 ($r \to \infty$). Ingoing Eddington-Finkelstein coordinates $\{\bar{v}, \sigma\}$ ensure that $\sigma \to \sigma_{\mathcal{H}}$ (along $\bar{v} = \text{const.}$) reaches the event horizon $\mathcal{H}$. Yet, the hypersurface $\sigma = 0$ (along $\bar{v} = \text{const.}$) corresponds to past null infinity $\mathscr{I}^-$. Indeed, the ingoing null vector $\tilde{k}^a$ points towards the interior of the domain, whereas $\tilde{l}^a$ is tangent to $\sigma = 0$ (cf. expressions (11)). In the hyperboloidal coordinates $\{\tau, \sigma\}$, the height function ensures that $\sigma = 0$ (along $\tau = \text{const.}$) corresponds to future null infinity $\mathscr{I}^+$, with $\tilde{k}^a \propto \delta^a_\tau$ and therefore tangent to $\sigma = 0$.

3. Comparison with Zenginoglu's scri-fixing prescription

We finish this section by comparing the approach/notation we used for the height function technique against the original one introduced in [12, 30]. First of all, the height function h here follows from (12) — i.e. a transformation from the ingoing Eddington-Finkelstein coordinate $\bar{v}$. Zenginoglu's height function h_{Z} is defined [12, 30] in terms of the original Schwarzschild coordinate t. Taking into account the correct signs and dimension re-scalings, we have

$$h_{\text{Z}} = -\left(r^* + \lambda h\right). \tag{27}$$

In [12], the geometric framework is discussed in terms of the boost function

$$H := \frac{\mathrm{d}h_{\text{Z}}}{\mathrm{d}r^*} = -1 + \frac{\sigma^2 F}{\beta} h'. \tag{28}$$

In particular, Eq. (2) in [12] specifies the conditions for the time-constant slices to be horizon-penetrating and hyperboloidal. Due to our preliminary step in terms of ingoing Eddington-Finkelstein coordinates, all conditions imposed on H as $r \to r_{\mathcal{H}}$ are automatically satisfied.

In a more general formulation, the work [30] discusses matching conditions that smoothly connect the asymptotic behavior of the hyperboloidal slices to Cauchy hypersurfaces in the interior of the spacetime [36]. Moreover, the areal radius ρ of the conformal spacetime is regarded as the new compact coordinate and the conformal factor $\Omega(\rho)$ is a free function. Here, we choose a compact coordinate naturally adapted to the conformal factor via $\sigma = \lambda \Omega$, whereas the areal radius $\rho(\sigma)$ is a free function fixing the gauge. The motivation in [30] to introduce the matching conditions and to let a free conformal factor $\Omega(\rho)$ arises from the considered objective of applying the hyperboloidal approach to solve numerically the full non-linear Einstein's equation[4].

In the context of perturbation theory, however, where the background spacetime is known *a priori*, adapting the radial coordinates to the conformal factor and fixing the function $A(\sigma) = 0$ simplifies significantly the equations under study. Thus, the *minimal gauge* reduces the complexity of the problem to a minimum, where $F(\sigma)$ is the only relevant function. In fact, the minimal gauge was employed beyond spherical symmetry in [46] in the numerical evolution of the Teukolsky equation in the Kerr spacetime. Even though the qualitative results do not differ from other studies (e.g. [47–51]), the analytical structure of the spacetime metric and the wave equation become much simpler.

III. SPECTRAL DECOMPOSITION FOR BLACK-HOLE PERTURBATIONS

A. Wave equation

1. Master wave equation

Black-hole perturbation theory is usually formulated in the Schwarzschild coordinate system $\{t, r, \theta, \phi\}$. Introducing di-

---

[4] See [37–45] for non-linear time evolutions in the context of hyperboloidal foliations.

mensionless coordinates $\bar{t} = t/\lambda$ and $x = r^*/\lambda$, one typically studies the wave equation

$$-\Psi_{,\bar{t}\bar{t}} + \Psi_{,xx} - \mathcal{P}\Psi = 0 \, . \tag{29}$$

The structure of equation (29) is generic in a large class of fields propagating on a spherical background. For instance, scalar, electromagnetic or gravitational perturbations differ only in the forms for the potential $\mathcal{P}$. A solution to this equation is uniquely determined once we impose the initial data

$$\Psi_0(x) = \Phi(0, x), \quad \dot{\Psi}_0(x) = \Psi_{,t}(0, x) \, , \tag{30}$$

together with (generally time-dependent) boundary conditions at inner $x = x_{\mathrm{in}}(t)$ and outer $x = x_{\mathrm{out}}(t)$ hypersurfaces. In particular, in the QNM setting, outgoing boundary conditions must be imposed at $x_{\mathrm{out}} \to +\infty$ and at $x_{\mathrm{in}} \to -\infty$. Note that in this particular Cauchy slicing foliated by $\bar{t} = $ constant, the limits $x_{\mathrm{out}} \to +\infty$ and $x_{\mathrm{in}} \to -\infty$ correspond to spatial infinity and the bifurcation sphere, respectively.

The coordinate changes (7) and (12) can be applied directly to Eq. (29). Let us introduce the factorization

$$\mathcal{P}(r) = \frac{\lambda^2}{r^2} f(r) \mathrm{P}(r) \, . \tag{31}$$

Firstly, the introduction of the compact ingoing Eddington-Finkelstein coordinates (7) leads to

$$-2\,\mathrm{v}_{,\bar{v}\sigma} + \left[\frac{\sigma^2 F}{\beta} \mathrm{v}_{,\sigma} \right]_{,\sigma} - \frac{\beta}{\rho^2} \mathrm{P}\,\mathrm{v} = 0 \, , \tag{32}$$

with $\mathrm{v}(\bar{v}, \sigma) = \Psi(t(\bar{v}, \sigma), r(\sigma))$.

When passing from (29) to (32), one can factor out the quantity $\sigma^2 F(\sigma)$, which vanishes at null infinity $\sigma = 0$ and at the horizon $F(\sigma_{\mathcal{H}}) = 0$. Yet, another factor of the form $\sigma^2 F(\sigma)$ is still present as the coefficient of $\mathrm{v}_{,\sigma\sigma}$ and the equation (32) degenerates at $\sigma = 0$ and $\sigma = \sigma_{\mathcal{H}}$. As a consequence of this latter feature, regularity conditions must be taken into consideration when solving the equation.

We recall that the intermediate step involving the ingoing Eddington-Finkelstein coordinates was only meant to enforce the horizon-penetrating property and to introduce the conformal compactification of the spacetime. The surface $\sigma = 0$ (along $\bar{v} = $ constant) corresponds to *past* null infinity $\mathscr{I}^-$, with the ingoing null vector k^a pointing towards the interior of the domain $\sigma > 0$ — see Eq. (11) (cf. also the right panel in figure 1 and footnote 3). At the partial differential equation level, the wave equation is formulated as a characteristic problem, for which a unique solution is obtained with the prescription of data at the null hypersurfaces $\bar{v} = 0$ and $\sigma = 0$.

With the introduction of the hyperboloidal slices (12), the limiting value $\sigma = 0$ is performed along $\tau = $ constant. In this case, the height function $h(\sigma)$ ensures that $\sigma = 0$ corresponds to *future* null infinity $\mathscr{I}^+$. The wave equation then reads

$$-2h'\left[1 - \frac{\sigma^2 F}{2\beta}h'\right]V_{,\tau\tau} - 2\left[1 - \frac{\sigma^2 F}{\beta}h'\right]V_{,\tau\sigma} + \frac{\sigma^2 F}{\beta}V_{,\sigma\sigma}$$
$$+ \left[\frac{\sigma^2 F}{\beta}\right]' V_{,\sigma} + \left[\frac{\sigma^2 F h'}{\beta}\right]' V_{,\tau} - \frac{\beta}{\rho^2}\mathrm{P}\, V = 0 \, , \tag{33}$$

with $V(\tau, \sigma) = \mathrm{v}(\bar{v}(\tau, \sigma), \sigma)$.

Despite the rather complicated form of Eq. (33), it is straightforward to see that the term proportional to $V_{,\sigma\sigma}$ still vanishes at both $\sigma = 0$ and $\sigma = \sigma_{\mathcal{H}}$, i.e. at future null infinity and at the black hole horizon.

At the boundaries $\sigma = 0$ and $\sigma = \sigma_{\mathcal{H}}$, the characteristics of the system never point inwards the domain $\sigma \in [0, \sigma_{\mathcal{H}}]$ (cf. the left panel in figure 1). Therefore, the wave equation is treated as a Cauchy problem for which the prescription of initial data

$$V_0(\sigma) = V(0, \sigma) \quad \text{and} \quad \dot{V}_0(\sigma) = V_{,\tau}(0, \sigma) \, , \tag{34}$$

is sufficient to fix uniquely the time solution for $\tau > 0$. In sharp contrast with the Cauchy formulation in terms of the original Schwarzschild coordinates $\{t, r, \theta, \varphi\}$, no further boundary conditions are required.

Note however, that this procedure is based on a direct change of coordinates applied to the master equation (29). A more systematic geometrical approach should be based on a coordinate independent formulation according to the conformal transformation of the spacetime $g_{ab} = \Omega^{-2}\tilde{g}_{ab}$. In the next section we discuss this procedure for the scalar field. A complete conformal treatment of electromagnetic and gravitational perturbations is beyond the scope of this work.

2. Conformal wave equation

We start with the conformally invariant wave equation [52] for a massless scalar field $U(t, r, \theta, \varphi)$ propagating in the background provided by the metric g_{ab}

$$\Box U - \frac{R}{6}U = 0 \, , \tag{35}$$

with R the Ricci scalar associated with the metric g_{ab}. Here, we are particularly interested in spacetimes satisfying $R = 0$.

Note that Eq. (29) is recovered with the decomposition[5]

$$U(t, r, \theta, \varphi) = \sum_{\ell, m} \frac{\Psi_{\ell,m}(t, r)}{r} Y_{\ell,m}(\theta, \varphi) \, . \tag{36}$$

In particular, the potential is given by

$$\mathrm{P}(r) = \ell(\ell+1) + r\, f'(r) \, . \tag{37}$$

In terms of the conformal metric $\tilde{g}_{ab}$, the conformally rescaled scalar field $\tilde{U}$ satisfies

$$\tilde{\Box}\tilde{U} - \frac{\tilde{R}}{6}\tilde{U} = 0 \, , \quad \tilde{U} = \Omega^{-1}U \, , \tag{38}$$

with

$$\tilde{R} = -\frac{6}{\Omega}\left[\tilde{\Box}\Omega - 2\frac{\tilde{\nabla}_a\Omega\tilde{\nabla}^a\Omega}{\Omega}\right] = -\frac{6\sigma}{\beta\rho^2}\left[\frac{\rho^2 F}{\beta}\right]' \, , \tag{39}$$

---

[5] For simplicity, the indices $_{\ell,m}$ were absent in Eq. (29), (32) and (33).

the Ricci scalar associated with the metric $\tilde{g}_{ab}$. With the decomposition

$$\tilde{U}(\tau,\sigma,\theta,\varphi) = \sum_{\ell,m} \Phi_{\ell,m}(\tau,\sigma) Y_{\ell,m}(\theta,\varphi) , \qquad (40)$$

we obtain

$$-2h'\left[1 - \frac{\sigma^2 F}{2\beta}h'\right]\Phi_{,\tau\tau} - 2\left[1 - \frac{\sigma^2 F}{\beta}h'\right]\Phi_{,\tau\sigma} + \frac{\sigma^2 F}{\beta}\Phi_{,\sigma\sigma}$$

$$+\frac{1}{\rho^2}\left[\frac{\sigma^2\rho^2 F}{\beta}\right]'\Phi_{,\sigma} - \frac{1}{\rho}\left[2\rho' - \frac{(\sigma^2\rho^2 Fh'/\beta)'}{\rho}\right]\Phi_{,\tau}$$

$$-\frac{\beta}{\rho^2}\tilde{\mathcal{P}}\,\Phi = 0 . \qquad (41)$$

Here, the potential reads

$$\tilde{\mathcal{P}} = \ell(\ell+1) - \frac{\sigma}{\beta}\left[\frac{\rho^2 F}{\beta}\right]' . \qquad (42)$$

Inserting Eqs. (36) and (40) into (38) — and then using (7) and (10) — the conformally re-scaled scalar field Φ relates to V via

$$V(\tau,\sigma) = \rho(\sigma)\Phi(\tau,\sigma) . \qquad (43)$$

If $\rho(\sigma) = \text{constant}$, there is no distinction between changing variables of the original master equation (29) into (33), as done in the previous subsection III A 1, and writing the conformally invariant wave equation (41). Otherwise, the wave operator differs. In particular, in the minimal gauge[6], $\rho(\sigma)$ is an affine function of σ (cf. Eq. (24)). In this setting, we privilege the conformally invariant wave equation as the natural choice, due to its geometrical formulation.

Deriving a conformally invariant master equation in a more generic setup including, for instance, electromagnetic and gravitational perturbation should be the topic of future works. Yet, we expect to relate a conformally re-scaled perturbation $\Phi(\tau,\sigma)$ to the well-known formulation in terms of a field $\Psi(\bar{t},x)$ satisfying an equation in the form of Eq. (29) via a re-scaling

$$\Psi(t(\tau,\sigma), r(\sigma)) \equiv V(\tau,\sigma) = \rho(\sigma)^n \Phi(\tau,\sigma) , \qquad (44)$$

with n depending on the type of field.

We apply this assumption to Eq. (33) in order to obtain a general form for the "conformal" wave equation

$$-2h'\left[1 - \frac{\sigma^2 F}{2\beta}h'\right]\Phi_{,\tau\tau} - 2\left[1 - \frac{\sigma^2 F}{\beta}h'\right]\Phi_{,\tau\sigma} + \frac{\sigma^2 F}{\beta}\Phi_{,\sigma\sigma}$$

$$+\frac{1}{\rho^{2n}}\left[\frac{\sigma^2\rho^{2n}F}{\beta}\right]'\Phi_{,\sigma} - \left[2n\frac{\rho'}{\rho} - \frac{(\sigma^2\rho^{2n}Fh'/\beta)'}{\rho^{2n}}\right]\Phi_{,\tau}$$

$$-\frac{\beta}{\rho^2}\tilde{\mathcal{P}}\,\Phi = 0 . \qquad (45)$$

---

[6] Note that the whole discussion in subsection III A 1 is independent of the gauge choice for $\rho = \rho(\sigma)$ and $h = h(\sigma)$. Eqs. (32) and (33), as well as (41), apply therefore in the generic case, and not only in the *minimal gauge*.

While the potential in Eq. (42) has a geometrical meaning in terms of the conformal Ricci scalar $\tilde{R}$, here we simply define it as

$$\tilde{\mathcal{P}} = \text{P} - \frac{\rho^{2-n}}{\beta}\left[\frac{\sigma^2 F}{\beta}(\rho^n)'\right]' . \qquad (46)$$

Eq. (43) provides naturally the value $n = 1$ to scalar perturbations. In section V we study a concrete example of electromagnetic and gravitational perturbations on the Reissner-Nordström spacetime. There, we identify the value $n = -1$ for such fields. It is tempting to speculate that the scaling $n = -1$ should follow naturally if one formulates *ab initio* the master equation for electromagnetic and gravitational perturbations within the conformal representation of the spacetime.

B. Laplace Transformation

We now proceed as in [11] and introduce the Laplace transformation

$$\hat{\Phi}(\sigma;s) := \mathcal{L}[\Phi(\tau,\sigma)](s) = \int_0^\infty e^{-s\tau}\Phi(\tau,\sigma)\,\mathrm{d}\tau , \ \Re(s) > 0 . \qquad (47)$$

Applying the Laplace transformation to Eq. (45) leads to the ordinary differential equation (ODE)

$$\mathbf{A}(s)\hat{\Phi}(s) = B(s) , \qquad (48)$$

with

$$\mathbf{A}(s) = \frac{\sigma^2 F}{\beta}\partial_{\sigma\sigma} + \left(\frac{1}{\rho^{2n}}\left[\frac{\sigma^2\rho^{2n}F}{\beta}\right]' - 2s\left[1 - \frac{\sigma^2 F}{\beta}h'\right]\right)\partial_\sigma$$

$$-\left(\frac{\beta}{\rho^2}\tilde{\mathcal{P}} + s\left[2n\frac{\rho'}{\rho} - \frac{(\sigma^2\rho^{2n}Fh'/\beta)'}{\rho^{2n}}\right] + 2s^2 h'\left[1 - \frac{\sigma^2 F}{2\beta}h'\right]\right) \qquad (49)$$

and

$$B(s) = -2h'\left[1 - \frac{\sigma^2 F}{2\beta}h'\right]\left(s\Phi_0 + \dot{\Phi}_0\right) - 2\left[1 - \frac{\sigma^2 F}{\beta}h'\right]\Phi_{0,\sigma}$$

$$-\left[2n\frac{\rho'}{\rho} - \frac{(\sigma^2\rho^{2n}Fh'/\beta)'}{\rho^{2n}}\right]\Phi_0 , \qquad (50)$$

where $\Phi_0(\sigma) = \Phi(0,\sigma)$ and $\dot{\Phi}_0 = \partial_\tau\Phi(0,\sigma)$ are the initial data for the wave equation (45).

1. Comparison with the Cauchy formulation

Let us relate the operator $\mathbf{A}(s)$ on the hyperboloidal slice to the corresponding one on Cauchy slices $\bar{t} = \text{constant}$. First we write the Laplace transform of the field $\Psi(\bar{t},x)$ with re-

spect to the parameter $\bar{t}$ [7]

$$\hat{\Psi}(x;s) := \mathcal{L}[\Psi(\bar{t},x)](s) = \int_0^\infty e^{-s\bar{t}} \Psi(\bar{t},x)\,\mathrm{d}\bar{t}\,. \quad (51)$$

Applying the Laplace transformation to the wave equation (29) leads to the standard formulation

$$\mathcal{D}(s)\hat{\Psi}(s) = S(s)\,, \quad (52)$$

with

$$\mathcal{D}(s) = \partial_{xx} - (s^2+\mathcal{P})\,, \quad S(s) = -\dot{\Psi}_0(x) - s\Psi_0(x)\,. \quad (53)$$

As stated in Eq. (30), $\Psi_0(x)$ and $\dot{\Psi}_0(x)$ are the initial data at the *Cauchy* slice $\bar{t} = 0$. Note that such functions are defined on a different time slice as compared to functions $\Phi_0(\sigma)$ and $\dot{\Phi}(\sigma)$, which are defined in the hyperboloidal slice $\tau = 0$.

Taking into account the relation derived from (7) and (12)

$$\tau = \bar{t} + x + h(\sigma(x))\,, \quad (54)$$

the factor $e^{-s\tau}$ in the Laplace transform of $V(\tau,\sigma)$ writes as $e^{-s(x+h)}e^{-s\bar{t}}$. This result, together with the conformal rescaling (44), motivates the introduction of the factor

$$Z(x;s) := \rho(\sigma(x))^n e^{s(x+h)}\,, \quad (55)$$

to relate the Laplace transforms with respect to τ and $\bar{t}$, and therefore the action of the operators $\mathbf{A}(s)$ and $\mathcal{D}(s)$. Specifically, for functions $\psi(x;s)$ and $\phi(\sigma;s)$ related as

$$\psi(x;s) = Z(x;s)\phi(\sigma(x);s)\,, \quad (56)$$

it holds

$$\mathcal{D}(s)\psi(s) = \frac{Z\sigma^2 F}{\beta}\mathbf{A}(s)\phi(s)\,. \quad (57)$$

In studies starting from the homogeneous equation $\mathcal{D}(s)\psi(s) = 0$, such a rescaling factor Z is introduced after an asymptotic study of the ODE (and a bit of algebra) as a way of imposing the desired outgoing boundary conditions leading to QNMs [8] [29, 53]. In the present discussion, it follows clean and directly from the geometrical considerations of the hyperboloidal slices.
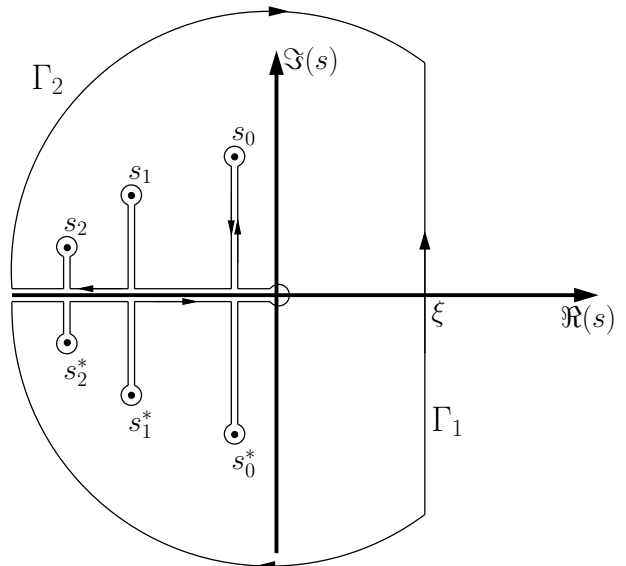
––––––––––

[7] In principle one should distinguish the spectral parameter $\bar{s}$ associated with the Laplace transform in terms of $\bar{t}$ from the parameter s employed for the transformation in terms of τ. However, such spectral parameters coincide since both $\bar{t}$ and τ are natural parameters of the timelike Killing vector $\xi = \lambda\partial_t$, namely $\xi(\bar{t}) = \xi(\tau) = 1$ (actually $\xi = \partial_{\bar{t}} = \partial_\tau$).

[8] The concept of outgoing boundary conditions leading to QNMs is often expressed solely as $\psi(x;s) \sim e^{\mp sx}$ for $x \to \pm\infty$. Though necessary, such conditions are not sufficient — see e.g. section 3.1.2 in [3] and references therein. Indeed, in [11] regular solutions to the wave equation are constructed with arbitrary decay and frequency time scales.

FIG. 2. Integration paths for the inverse Laplace transformation. The Bromwich integral (58) is evaluated along the line Γ_1 in the right-plane $\Re(s) > 0$ (taking its upper and lower limits to $+\infty$ and $-\infty$, respectively). The spectral decomposition (2) is formally obtained from the Cauchy theorem with the deformation of the path and integration along the curve $\Gamma_1 - \Gamma_2$.

C. Spectral decomposition

The solution to the time evolution $\Phi(\tau,\sigma)$ is formally obtained via the inverse Laplace transformation (Bromwich Integral)

$$\Phi(\tau,\sigma) = \frac{1}{2\pi i}\int_{\Gamma_1}\hat{\Phi}(\sigma;s)e^{s\tau}\,\mathrm{d}s\,, \quad (58)$$

with the integration path

$$\Gamma_1 = \{s \in \mathbb{C}\,|\,s = \xi + i\chi, \xi > 0, \chi \in (-\infty,+\infty)\}\,. \quad (59)$$

The spectral decomposition (2) is obtained by (maximally) analytically extending the function $\hat{V}(\sigma;s)$ into the half-plane $\Re(s) < 0$ and then appropriately deforming the path Γ_1 into that semi-plane — see Fig. 2.

When deforming the Bromwich integration path from Γ_1 to Γ_2, we gather a contribution from the QNMs s_n, the branch cut along the negative real axis $s \in \mathbb{R}^-$ and, in principle, the external semicircle, following the discussion in [11, 54, 55]. In particular, [11] presents a detailed description of the algorithm and its application to the Schwarzschild case leading to

$$\Phi(\tau,x^k) = \sum_{n=0}^\infty \eta_n e^{s_n\tau}\phi_n(x^k) + \int_{-\infty}^0 \eta(s)e^{s\tau}\phi(x^k;s)ds$$

and conjecture 1.

In next section IV, we present a more general procedure to calculate all the needed ingredients in the spectral decomposition, namely: i) the QNM frequencies s_n together with the

functions $\phi_n(x^k)$ and $\phi(x^k, x)$, and ii) the QNM and branch cut amplitudes, respectively, η_n and $\eta(s)$. The former are elements intrinsic to the wave equation, whereas the latter depend on the initial data.

IV. ALGORITHM IN FREQUENCY SPACE

A. Taylor series expansions

In [11], Eq. (48) was solved in the Schwarzschild background via a non-trivial Taylor series expansions around the horizon $\sigma = \sigma_{\mathcal{H}}$. Here, we generalize this procedure to an arbitrary asymptotically flat spherically symmetric spacetime.

1. Homogeneous Equations

We first consider the homogeneous Laplace transformed equation

$$\mathbf{A}(s)\phi(s) = 0 . \quad (60)$$

In a first step, we focus on solutions which are analytic in a neighborhood around the horizon $\mathcal{H}$, gauge fixed in section II C 2 to $\sigma_{\mathcal{H}} = 1$. Thus, we expand $\phi(s)$ in terms of a Taylor series

$$\phi(\sigma; s) = \sum_{k=0}^{\infty} H_k u^k , \quad u = 1 - \sigma . \quad (61)$$

Singular points of this ODE are given by $\sigma = 0$ and $\sigma = \infty$, as well as by the values $\sigma = \sigma_{\mathrm{H}_j}$, such that $F(\sigma_{\mathrm{H}_j}) = 0$. The smallest real root represents the event horizon $\mathcal{H}$, therefore it must hold $\sigma_{\mathrm{H}_0} = 1$ in the adopted gauge.

Given the unit circle

$$\mathbf{C} = \{\sigma \in \mathbb{C} : |1 - \sigma| < 1\} , \quad (62)$$

a necessary condition for the convergence of the series (61) within $\mathbf{C}$ (and therefore up to the vicinity of future null infinity at $\sigma = 0$) requires that further (eventually complex) roots of $F(\sigma)$ lie outside $\mathbf{C}$. In the particular case of Reissner-Nordström, the (real) root σ_1 associated with the Cauchy horizon must satisfy $\sigma_{\mathrm{H}_1} \geq 2$.

In the minimal gauge (see section II C 2), the coefficients of the operator $\mathbf{A}(s)$ are polynomials [9] in σ. Therefore, the introduction of the Ansatz (61) into (60) gives rise to a $(m + 2)$-term recurrence relation, i.e. a $(m + 1)$-order recurrence relation

$$\alpha_k H_{k+1} + \sum_{i=0}^{m} \beta_k^{(i)} H_{k-i} = 0 , \quad k \geq m , \quad (63)$$

with $m \in \mathbb{N}$, $\alpha_{-1} = 0$ and the coefficients α_k and $\beta_k^{(i)}$ depending on the structure of the operator $\mathbf{A}(s)$ (see Eq. (49) and also (153) below for an illustration in the Reissner-Nordström case).

The $m + 1$ initial values H_k ($k = 0, \dots, m$) needed to iterate (63) must satisfy (a suitable normalization is $H_0 = 1$)

$$\alpha_k H_{k+1} + \sum_{i=0}^{k} \beta_k^{(i)} H_{k-i} = 0 , \quad k = 0, \dots, m - 1 . \quad (64)$$

These constraints follow from extending the validity of the relation (63) to $k = 0, \dots, m - 1$ and imposing

$$H_{-k} = 0, \quad k = 1, \dots, m . \quad (65)$$

Note that (65) applied to (63) for $k < 0$ automatically ensures $H_k = 0$ for all $k < 0$, i.e., the constraints (64) encode the information about the regularity of (61) at $\sigma = 1$.

Let us now relax the conditions imposed by the constraints (64) — or equivalently, by (65) — and construct all the $m + 1$ linearly independent sequences $\{H_k^{(\ell)}\}_{k=-m}^{\infty}$ ($\ell = 0, \dots, m$) satisfying

$$H_{-k}^{(\ell)} = \delta_k^\ell , \quad k = 0, \dots, m \quad (66)$$

$$\alpha_k H_{k+1}^{(\ell)} + \sum_{i=0}^{m} \beta_k^{(i)} H_{k-i}^{(\ell)} = 0 , \quad k \geq 0 , \quad (67)$$

with δ_k^ℓ the Kronecker delta. For $\ell = 0$, Eqs. (66) and (67) recover (63)-(65), i.e., the sequence $\{H_k^{(0)}\}_{k=-m}^{\infty}$ corresponds to the Taylor coefficients leading to (61).

We consider now the asymptotic behavior of (67) for large k values. From the findings in [11, 29, 53, 56], we consider the cases where H_k behaves asymptotically as[10]

$$H_k \sim e^{\xi k^p} k^\zeta A_k , \quad A_k = 1 + \sum_{j=1}^{\infty} \frac{\nu_j}{k^{jp}} \quad (68)$$

with $p = 1/2$ or $p = 1$.

For a fixed asymptotic parameter p, an algorithm to determine the coefficients ξ, ζ and $\{\nu_j\}_{j=1}^{\infty}$ consists in (i) inserting (68) back into the recurrence relation (63), (ii) multiplying the result by $e^{-\xi k^p} k^{-\zeta}$, (iii) expanding the resulting expression in terms of $y = k^{-p}$ around $y = 0$, and (iv) equating the coefficients of the asymptotic expansion order by order [11].

From the perspective of the asymptotic expansion, the freedom to construct the $m + 1$ linearly independent solutions is captured by the existence of $m + 1$ asymptotic coefficients $\xi^{(\ell)}$, $\zeta^{(\ell)}$ and $\{\nu_j^{(\ell)}\}_{j=1}^{\infty}$ ($\ell = 0, \dots, m$). Thus, the asymptotic

---

[9] One might need to multiply the equation by an appropriate power of ρ, in case $\rho(\sigma)$ is not a constant but presents a linear term in σ — see Eq. (24).

[10] The assumptions until the end of this section are corroborated by the scenarios studied in [11, 15, 57, 58]. A more rigorous statement relating such behaviors, the (polynomial in k) form of the coefficients α_k, $\beta_k^{(i)}$ and the convergence region given by the unit circle $\mathbf{C}$ requires further work that goes beyond the scope of this paper.

behavior of each sequence $\{H_k^{(\ell)}\}_{k=-m}^{\infty}$ is given by a linear combination

$$H_k^{(\ell)} \sim \lambda_{(0)}^{(\ell)} e^{\xi^{(0)} k^{p^{(0)}}} k^{\zeta^{(0)}} A_k^{(0)} + \ldots$$
$$+ \lambda_{(\ell)}^{(\ell)} e^{\xi^{(m)} k^{p^{(m)}}} k^{\zeta^{(m)}} A_k^{(m)} , \qquad (69)$$

with $\lambda_{\ell'}^{\ell}$ generic coefficients.

We also assume that $\left| e^{\xi^{(0)}} \right| > 1$, whereas, for $\ell = 1, \ldots, m$, $\left| e^{\xi^{(\ell)}} \right| < 1$, i.e., the asymptotic (0)-mode grows for large k while the (ℓ)-modes ($\ell = 1, \ldots, m$) decay. Moreover, we label the asymptotic parameters in such a way that

$$0 < \left| e^{\xi^{(m)}} \right| \le \left| e^{\xi^{(m-1)}} \right| \le \ldots \le \left| e^{\xi^{(1)}} \right| < 1 . \qquad$$

Note that the sequences $\{H_k^{(\ell)}\}_{k=-m}^{\infty}$ are obtained according to (67), by fixing their initial seeds via (66). When iterating (67) forwardly, we cannot control the asymptotic behavior and, in general, the growing mode will dominate. Our aim is to introduce a new set of linear independent sequences $\{I_k^{(\ell)}\}_{k=-m}^{\infty}$ still satisfying the recurrence relation (67), but also eliminating the growing asymptotic behavior[11].

For this task, we first identify directly $H_k^{(0)} = I_k^{(0)}$, i.e., $I_k^{(0)}$ satisfies, on the one hand, the constraints (64) needed for the regularity properties of (60) at $\sigma = 1$ and, on the other hand, it generically grows asymptotically as $\sim e^{\xi^{(0)} k^{p^{(0)}}} k^{\zeta^{(0)}}$. Then, we successively filter the asymptotic modes by defining

$$I_k^{(\ell)} = \sum_{\ell'=0}^{\ell} \kappa_{\ell'}^{(\ell)} H_k^{(\ell')}, \qquad (\ell = 1, \ldots, m) . \qquad (70)$$

For each $\ell = 1, \ldots, m$, there are $(\ell + 1)$ constants $\kappa_{\ell'}^{(\ell)}$ to be fixed. To determine such constants, we prescribe a truncation $k_{\max}$ and consider (70) at $(\ell + 1)$ values $k = k_{\max} + l$ ($l = 0, \ldots, \ell$). The asymptotic behavior of $I_{k_{\max}+l}^{(\ell)}$ is then approximated via the algorithm from [11] applied to the desired decaying behavior $\sim e^{\xi^{(\ell)} k^{p^{(\ell)}}} k^{\zeta^{(\ell)}}$. This procedure provides us with $(\ell + 1)$ equations to fix $\kappa_{\ell'}^{(\ell)}$. Having imposed the desired decaying behavior to the sequence $\{I_k^{(\ell)}\}_{k=-m}^{\infty}$, we normalize it to $I_0^{(\ell)} = 1$ by letting $I_k^{(\ell)} \to I_k^{(\ell)}/I_0^{(\ell)}$.

Summarizing the discussion above, we have constructed $(m + 1)$ linearly independent sequences $\{I_k^{(\ell)}\}_{k=-m}^{\infty}$ ($\ell = 0, \ldots, m$) which are solutions to the recurrence relation (67) and satisfy:

(1) There is *one* specific solution $I_k^{(0)}$ with

$$I_k^{(0)} = 0 \quad \text{for} \quad k < 0 . \qquad (71)$$

(2) As $k \to \infty$, the coefficients $I_k^{(\ell)}$ decay for $\ell = 1, \ldots, m$. In contrast, the coefficients $I_k^{(0)}$ are assumed to diverge as $k \to \infty$.

The solutions $I_k^{(\ell)}$ ($\ell = 1, \ldots, m$) are refereed to as *decaying* solutions.

(3) For all $\ell = 0, \ldots, m$, the sequences are normalized to

$$I_0^{(\ell)} = 1 . \qquad (72)$$

(4) For the first few negative indices $-m \le k < -\ell$, the decaying solutions $I_k^{(\ell)}$ ($\ell = 1, \ldots, m$) satisfy

$$I_k^{(\ell)} = 0 . \qquad (73)$$

2. Inhomogeneous equation

We now proceed to the general algorithm to solve the Laplace transformed equation (48). According to the previous section, we seek a solution $\hat{\Phi}(\sigma; s)$ of the form

$$\hat{\Phi}(\sigma; s) = \sum_{k=0}^{\infty} a_k (1 - \sigma)^k . \qquad (74)$$

The coefficients a_k satisfy the inhomogeneous recurrence relation

$$\alpha_k a_{k+1} + \sum_{i=0}^{m} \beta_k^{(i)} a_{k-i} = q_k , \qquad (75)$$

with q_k the coefficients for the expansion of the source (50)

$$B(\sigma; s) = \sum_{k=0}^{\infty} q_k (1 - \sigma)^k . \qquad (76)$$

As in [11], we initially consider an inhomogeneity of polynomial kind, i.e., with

$$q_k = 0 \quad \text{for} \quad k < 0 \quad \text{and} \quad k > K_{\max} . \qquad (77)$$

The analytic limit $K_{\max} \to \infty$ is taken in the end of this section. Finally, we restrict ourselves to regular solutions satisfying

$$\begin{cases} a_k = 0 & \text{for} \quad k < 0 \\ a_k \to 0 & \text{as} \quad k \to \infty . \end{cases} \qquad (78)$$

We seek the solution a_k to the inhomogeneous recurrence relation in the form

$$a_k = \sum_{\ell=0}^{m} c_{k,\ell} I_k^{(\ell)} , \qquad (79)$$

i.e., as a linear combination of the solutions $I_k^{(\ell)}$ to the homogeneous relation. In order to fix the coefficients $c_{k,\ell}$ we must

---

[11] In [11], this procedure is done via a backward iteration of the recurrence relation. Appendix VII B discusses this strategy in the current context.

impose, together with (75), m further conditions. In particular, the conditions

$$\sum_{\ell=0}^{m} c'_{k,\ell} I^{(\ell)}_{k-p} = 0, \quad p = 0, \ldots, m-1 , \tag{80}$$

extend Eq. (64) in [11] to the present general case. Eqs. (79) and (80) constitute the generalization of the Ansatz in [11] for the solution of the recurrence relation.

In order to justify (80), we introduce the discrete derivative

$$c'_{k,\ell} = c_{k+1,\ell} - c_{k,\ell} . \tag{81}$$

As a consequence, we find that

$$c_{k+1,\ell} = c_{k,\ell} + c'_{k,\ell}$$
$$c_{k-i,\ell} = c_{k,\ell} - \sum_{j=1}^{i} c'_{k-j,\ell} \quad (i \geq 1) . \tag{82}$$

The first one recasts the definition (81), whereas the second one follows again from such definition by writing

$$\sum_{j=1}^{i} c'_{k-j,\ell} = \sum_{j=1}^{i} c_{k-j+1,\ell} - \sum_{j=1}^{i} c_{k-j,\ell} ,$$

and shifting the index $j' = j - 1$ in the first sum of the right-hand-side to get

$$\sum_{j=1}^{i} c'_{k-j,\ell} = \sum_{j'=0}^{i-1} c_{k-j',\ell} - \sum_{j=1}^{i} c_{k-j,\ell} = c_{k,\ell} - c_{k-i,\ell} .$$

Combining these partial results with the Ansatz (79) we may write

$$a_{k+1} = \sum_{\ell=0}^{m} c_{k,\ell} I^{(\ell)}_{k+1} + \sum_{\ell=0}^{m} c'_{k,\ell} I^{(\ell)}_{k+1} \tag{83}$$

$$a_{k-i} = \sum_{\ell=0}^{m} c_{k,\ell} I^{(\ell)}_{k-i} - \sum_{j=1}^{i} \left(\sum_{\ell=0}^{m} c'_{k-j,\ell} I^{(\ell)}_{k-i} \right). \tag{84}$$

If we now impose, for *all* $k \in \mathbb{Z}$

$$a_{k-i} = \sum_{\ell=0}^{m} c_{k,\ell} I^{(\ell)}_{k-i} , \tag{85}$$

we must require, for $j = 1, \ldots, i$, the following relation to hold

$$\sum_{\ell=0}^{m} c'_{k-j,\ell} I^{(\ell)}_{k-i} = \sum_{\ell=0}^{m} c'_{k',\ell} I^{(\ell)}_{k'-(i-j)} = 0 ,$$

with $k' = k - j$. Thus, the m supplementary conditions (80) necessary to determine the coefficients $c_{k,\ell}$, uniquely follow from the expression above for $i = 1, \ldots, m$.

A key element in the algorithm in [11] is the introduction of a discrete Wronskian determinant associated with two numerical sequences $\{a_k\}^{\infty}_{-\infty}$ and $\{b_k\}^{\infty}_{-\infty}$ (cf. Eq. (55) in [11]).

We are now in position to generalize such a discrete Wronskian determinant to a set of $m + 1$ numerical sequences, as required in the present generalized setting [12]. We insert (83) and (85) into the original recurrence relation (75) to get

$$\sum_{\ell=0}^{m} c_{k,\ell} \left[\alpha_k I^{(\ell)}_{k+1} + \sum_{i=0}^{m} \beta_k^{(i)} I^{(\ell)}_{k-i} \right] + \alpha_k \sum_{\ell=0}^{m} c'_{k,\ell} I^{(\ell)}_{k+1} = q_k .$$

Since $I^{(\ell)}_k$ satisfies the homogeneous recurrence relation (63), this expression reduces to

$$\alpha_k \sum_{\ell=0}^{m} c'_{k,\ell} I^{(\ell)}_{k+1} = q_k . \tag{86}$$

The combination of Eqs. (80) and (86) leads to

$$\hat{\mathcal{W}}_k \begin{pmatrix} c'_{k,0} \\ c'_{k,1} \\ c'_{k,2} \\ \vdots \\ c'_{k,m} \end{pmatrix} = \begin{pmatrix} q_k/\alpha_k \\ 0 \\ 0 \\ \vdots \\ 0 \end{pmatrix} , \tag{87}$$

with the matrix $\hat{\mathcal{W}}_k$ defined by

$$\hat{\mathcal{W}}_k := \begin{pmatrix} I^{(0)}_{k+1} & I^{(1)}_{k+1} & \cdots & I^{(m)}_{k+1} \\ I^{(0)}_{k} & I^{(1)}_{k} & \cdots & I^{(m)}_{k} \\ I^{(0)}_{k-1} & I^{(1)}_{k-1} & \cdots & I^{(m)}_{k-1} \\ \vdots & \vdots & \ddots & \vdots \\ I^{(0)}_{k-(m-1)} & I^{(1)}_{k-(m-1)} & \cdots & I^{(m)}_{k-(m-1)} \end{pmatrix} . \tag{88}$$

This matrix provides us with a general definition for the discrete Wronskian determinant, namely

$$W_k = \det \hat{\mathcal{W}}_k . \tag{89}$$

Let us further define the sub-matrix $\hat{\mathcal{W}}_{k,\ell}$ as the one resulting from $\hat{\mathcal{W}}_k$ after removing the first row and the column $(I^{(\ell)}_{k+1} I^{(\ell)}_{k} \cdots I^{(\ell)}_{k-(m+1)})^T$, i.e.

$$\underbrace{\begin{pmatrix} I^{(0)}_{k} & \cdots & I^{(\ell-1)}_{k} & I^{(\ell+1)}_{k} & \cdots & I^{(m)}_{k} \\ I^{(0)}_{k-1} & \cdots & I^{(\ell-1)}_{k-1} & I^{(\ell+1)}_{k-1} & \cdots & I^{(m)}_{k-1} \\ \vdots & \ddots & \vdots & \vdots & \ddots & \vdots \\ I^{(0)}_{k-(m-1)} & \cdots & I^{(\ell-1)}_{k-(m-1)} & I^{(\ell+1)}_{k-(m-1)} & \cdots & I^{(m)}_{k-(m-1)} \end{pmatrix}}_{=:\hat{\mathcal{W}}_{k,\ell}} .$$

$$\tag{90}$$

---

[12] We assume that neither α_k nor $\beta_k^{(m)}$ vanish for a given integer k. Appendix C in [11] discusses the modifications in the algorithm accounting for such cases in $2-$order recurrence relations. Its generalization for a $m + 1$-order recurrence relations is actually relevant in scenarios involving odd-dimensional spacetimes, indeed a subject of current work [58].

Analogously to Eq. (89)

$$W_{k,\ell} = \det \hat{\mathcal{W}}_{k,\ell} . \qquad (91)$$

With the help of Eqs. (87)-(91) we are now able to write down an explicit expression for the solution a_k.

We begin by deriving a compact expression for the Wronskian determinant. First we define

$$\hat{\mathcal{W}}_k^\alpha := \begin{pmatrix} \alpha_k I_{k+1}^{(0)} & \alpha_k I_{k+1}^{(1)} & \cdots & \alpha_k I_{k+1}^{(m)} \\ I_k^{(0)} & I_k^{(1)} & \cdots & I_k^{(m)} \\ I_{k-1}^{(0)} & I_{k-1}^{(1)} & \cdots & I_{k-1}^{(m)} \\ \vdots & \vdots & \ddots & \vdots \\ I_{k-(m-1)}^{(0)} & I_{k-(m-1)}^{(1)} & \cdots & I_{k-(m-1)}^{(m)} \end{pmatrix} ,$$

and

$$\hat{\mathcal{W}}_k^{\alpha\beta} := \mathbb{I}^\beta \hat{\mathcal{W}}_k^\alpha ,$$

with

$$\mathbb{I}^\beta := \begin{pmatrix} 1 & \beta_k^{(0)} & \beta_k^{(1)} & \cdots & \beta_k^{(m-1)} \\ 0 & 1 & 0 & \cdots & 0 \\ 0 & 0 & 1 & \cdots & 0 \\ \vdots & \vdots & \vdots & \ddots & \vdots \\ 0 & 0 & 0 & \cdots & 1 \end{pmatrix} .$$

Note that

$$\alpha_k W_k = \det \hat{\mathcal{W}}_k^\alpha = \det \hat{\mathcal{W}}_k^{\alpha\beta} . \qquad (92)$$

Now, since the $I_k^{(\ell)}$ satisfy the homogeneous recurrence relation, the first row of $\hat{\mathcal{W}}_k^{\alpha\beta}$ explicitly reads

$$\left\{ \alpha_k I_{k+1}^{(\ell)} + \sum_{i=0}^{m-1} \beta_k^{(i)} I_{k-i}^{(\ell)} \right\}_{\ell=0}^m = \left\{ -\beta_k^{(m)} I_{k-m}^{(\ell)} \right\}_{\ell=0}^m .$$

Thus, we obtain

$$\det \hat{\mathcal{W}}_k^{\alpha\beta} = -\beta_k^{(m)} \det \begin{pmatrix} I_{k-m}^{(0)} & I_{k-m}^{(1)} & \cdots & I_{k-m}^{(m)} \\ I_k^{(0)} & I_k^{(1)} & \cdots & I_k^{(m)} \\ I_{k-1}^{(0)} & I_{k-1}^{(1)} & \cdots & I_{k-1}^{(m)} \\ \vdots & \vdots & \ddots & \vdots \\ I_{k-(m-1)}^{(0)} & I_{k-(m-1)}^{(1)} & \cdots & I_{k-(m-1)}^{(m)} \end{pmatrix} = -\beta_k^{(m)} (-1)^m W_{k-1} . \qquad (93)$$

In the above expression, the determinant W_{k-1} comes about once we swap the 1st and 2nd row, thereafter the 2nd and 3rd row and so on, until the first row is shifted to being the very last one. At each swap, we gain a factor -1. Since there are in total m swaps in this $(m+1) \times (m+1)$ dimensional matrix, a final factor $(-1)^m$ appears as well.

Combining (92) with (93) gives the simple result

$$\alpha_k W_k = (-1)^{m+1} \beta_k^{(m)} W_{k-1} ,$$

and therefore the desired result

$$W_k = W_{-1} \prod_{j=0}^k (-1)^{m+1} \frac{\beta_j^{(m)}}{\alpha_j} . \qquad (94)$$

We proceed now to find the solution a_k. Thanks to the property (71) in assumption (1), the normalization (72) in assumption (3) and (73) in assumption (4), we obtain

$$W_{-1} = W_{-1,0} = \prod_{\ell=1}^m I_{-\ell}^{(\ell)} . \qquad (95)$$

Moreover, for $k \leq -2$, $W_k = 0$ and therefore the system (87) cannot be inverted. Still, we want to enforce (80) for *all* k. In particular, Eq. (80) reads for $k < 0$

$$\hat{\mathcal{W}}_{k,0} \begin{pmatrix} c'_{k,1} \\ c'_{k,2} \\ \vdots \\ c'_{k,m} \end{pmatrix} = \begin{pmatrix} 0 \\ 0 \\ \vdots \\ 0 \end{pmatrix} . \qquad (96)$$

If we assume that $\hat{\mathcal{W}}_{k,0}$ is invertible ($W_{k,0} \neq 0$), we may conclude[13] that for $\ell = 1, \ldots, m$

$$c'_{k,\ell} = 0 \quad (k < 0) \Rightarrow c_{k,\ell} = \bar{c}_\ell = \text{const.} \quad (k \leq 0) \quad (97)$$

The constants $\bar{c}_\ell$ can be determined from (79). Indeed, taking m negative k values yields a system of m equations to determine the $\bar{c}'_\ell s$. Since $a_k = 0$ for $k < 0$, and assuming the system to be invertible, we obtain simply

$$c_{k,\ell} = 0 \quad \text{for} \quad \ell = 1, \ldots, m \quad \text{and} \quad k \leq 0 . \qquad (98)$$

For $\ell = 0$ though, the $c_{k,0}$ with $k \leq 0$ are arbitrary and undetermined.

---

[13] The passage from the strict inequality $k < 0$ to $k \leq 0$ follows from the definition of $c'_{k,\ell}$ in Eq. (81).

We now concentrate on the solution of (87) for $k \geq 0$ with "initial conditions" $c_{0,\ell} = 0$ for $\ell = 1, \ldots, m$ and a free, undetermined parameter $c_{0,0}$. The solution of this system emerges through the Cramer's rule as

$$c'_{k,\ell} = (-1)^\ell \frac{q_k}{\alpha_k} \frac{W_{k,\ell}}{W_k} . \tag{99}$$

With $c_{0,\ell} = 0$ for $\ell = 1, \ldots, m$, we get from (82)

$$c_{k,0} = c_{0,0} + \sum_{j=0}^{k-1} \frac{q_j}{\alpha_j} \frac{W_{j,0}}{W_j} \tag{100}$$

$$c_{k,\ell} = (-1)^\ell \sum_{j=0}^{k-1} \frac{q_j}{\alpha_j} \frac{W_{j,\ell}}{W_j}, \quad \ell = 1, \ldots, m. \tag{101}$$

It then follows, from (79), that

$$a_k = I_k^{(0)} \left(c_{0,0} + \sum_{j=0}^{k-1} \frac{q_j}{\alpha_j} \frac{W_{j,0}}{W_j} \right)$$
$$+ \sum_{\ell=1}^{m} (-1)^\ell I_k^{(\ell)} \sum_{j=0}^{k-1} \frac{q_j}{\alpha_j} \frac{W_{j,\ell}}{W_j} . \tag{102}$$

The constant $c_{0,0}$ is determined by imposing (78). Since $q_k = 0$ for $k > K_{\max}$ and, according to assumption (2), $I_k^{(0)}$ diverges in this limit, we must have

$$c_{0,0} = -\sum_{j=0}^{K_{\max}} \frac{q_j}{\alpha_j} \frac{W_{j,0}}{W_j} . \tag{103}$$

Hence

$$a_k = -I_k^{(0)} \sum_{j=k}^{K_{\max}} \frac{q_j}{\alpha_j} \frac{W_{j,0}}{W_j} + \sum_{\ell=1}^{m} (-1)^\ell I_k^{(\ell)} \sum_{j=0}^{k-1} \frac{q_j}{\alpha_j} \frac{W_{j,\ell}}{W_j} . \tag{104}$$

In this expression, the $K_{\max}$ can be taken arbitrarily large and we account for that by considering the formal series obtained by letting $K_{\max} \to \infty$. Besides, we can explicitly substitute the expression for W_j according to (94) to get

$$a_k = \frac{1}{W_{-1}} \left(-I_k^{(0)} \sum_{j=k}^{\infty} q_j \Xi_{j,0} + \sum_{\ell=1}^{m} (-1)^\ell I_k^{(\ell)} \sum_{j=0}^{k-1} q_j \Xi_{j,\ell} \right), \tag{105}$$

with

$$\Xi_{k,\ell} = W_{k,\ell} \frac{(-1)^{m+1}}{\alpha_k} \prod_{j=0}^{k} \frac{\alpha_j}{\beta_j^{(m)}} . \tag{106}$$

B. Quasi-normal modes and amplitudes

In accordance to [11], the QNM frequencies s_n are specific values in the complex $s-$plane for which the procedure described in the previous section fails. According to (105), this occurs whenever W_{-1} vanishes. Specifically, and thanks to (95), this occurs when

$$I_{-1}^{(1)} = 0 . \tag{107}$$

This condition, together with property (4) in section IV A 1, leads to $I_k^{(1)} = 0$ for *all* $k < 0$. Thus, the two solutions $I_k^{(0)}$ and $I_k^{(1)}$ become linearly dependent. In fact, they coincide here due to the normalization (3).

Having identified the condition in the present setting for the location of the QNMs, which depends only on the wave equation in question and is a property of the spacetime alone, we proceed to calculate the QNM amplitudes and the jump function along the branch cut, resulting from the specific choice of initial data.

1. Discrete amplitudes

Let us first recall the simplified notation introduced in [11] for the recurrence relation (75)

$$\mathcal{A}(s) \cdot \{a_k\} = \{q_k\} , \tag{108}$$

with the operator $\mathcal{A}(s)$ defined by

$$[\mathcal{A}(s) \cdot \{a_k\}]_k := \alpha_k a_{k+1} + \sum_{i=0}^{m} \beta_k^{(i)} a_{k-i} . \tag{109}$$

Assuming that W_{-1} has simple poles at discrete values s_n, we may write

$$a_k(s) = \frac{\eta_n I_k^{(0)}}{s - s_n} + g_k(s) . \tag{110}$$

Furthermore, we introduce a second operator $\mathcal{C}_n$ via

$$\mathcal{C}_n(s) = \frac{\mathcal{A}(s) - \mathcal{A}(s_n)}{s - s_n} . \tag{111}$$

In the limit $s \to s_n$, the decompositions (110) and (111) together with the condition for homogeneous solutions, (63) lead to

$$\mathcal{A}(s_n) \cdot \{g_k\} = \{q_k\} - \eta_n \mathcal{C}_n(s_n) \cdot \{I_k^{(0)}\} . \tag{112}$$

For $s \neq s_n$, the $k = 0$ solution to (112), according to (105), would be

$$g_0 = -\frac{1}{W_{-1}} \sum_{j=0}^{\infty} (q_j - \eta_n C_j) \Xi_{j,0} , \tag{113}$$

with

$$C_j := \left[\mathcal{C}_n(s) \cdot \{I_k^{(0)}\} \right]_j . \tag{114}$$

Since $W_{-1} \to 0$ in the limit $s \to s_n$, a finite value for g_0 is obtained only if

$$\eta_n = \frac{\sum\limits_{j=0}^{\infty} q_j \Xi_{j,0}}{\sum\limits_{j=0}^{\infty} C_j \Xi_{j,0}} . \tag{115}$$

For a given set of initial data, the η_n are the amplitudes associated with each QNM s_n and Eq. (115) generalizes the result from [11].

2. Branch cut amplitude

We end this section by considering the situation in which we approach the negative real axis in the complex $s-$plane. Depending on whether we approach the axis from above or from below we might encounter different solutions for the inhomogeneous recurrence relation. We begin by defining

$$a_k^\pm = \lim_{\varepsilon \to 0} a_k(s \pm i|\varepsilon|) , \qquad (116)$$

and we assume the symmetry condition (with upper asterisk $*$ denoting complex conjugation)

$$a_k^- = [a_k^+]^* , \qquad (117)$$

that follows from $V(\tau, \sigma)$ being a real valued function.

Since the difference $d_k = a_k^+ - a_k^-$ satisfies the homogeneous recurrence relation and satisfies $d_k = 0$ for $k < 0$, it must be proportional to $I_k^{(0)}$, so we may write

$$d_k = a_k^+ - a_k^- = d_0 I_k^{(0)} . \qquad (118)$$

According to the $k = 0$ value in (105), we have

$$d_0 = -\sum_{j=0}^\infty q_j \left(\frac{\Xi_{j,0}^+}{W_{-1}^+} - \frac{\Xi_{j,0}^-}{W_{-1}^-} \right) . \qquad (119)$$

Apart from properties (1)-(4) mentioned previously, let us also assume that when getting to the negative real axis from above or from below[14]:

5. Only the values of $I_k^{(1)}$ are different;

6. The recurrence relation coefficients α_k and $\beta_k^{(\ell)}$ do *not* differ.

Then, the contribution at the branch cut is due to

$$D_j = \frac{W_{j,0}^+}{W_{-1}^+} - \frac{W_{j,0}^-}{W_{-1}^-} , \qquad (120)$$

which can be conveniently re-expressed in terms of a quantity $D_0^{(1)}$, defined as [15]

$$D_j^{(1)} = \frac{I_j^{(1)+}}{I_{-1}^{(1)+}} - \frac{I_j^{(1)-}}{I_{-1}^{(1)-}} = D_0^{(1)} I_j^{(0)} , \qquad (121)$$

----

[14] In the cases studied, this assumption has always been found to be realized.

[15] The last equality is valid because $D_j^{(1)}$ satisfies the homogeneous recurrence relation with $D_k^{(1)} = 0$ for $k < 0$.

with

$$D_0^{(1)} = 2i \, \Im \left(\frac{I_0^{(1)+}}{I_{-1}^{(1)+}} \right) . \qquad (122)$$

To show the specific relation between D_j and $D_0^{(1)}$, we first write the determinant $W_{j,0}$ in Eq. (91) explicitly as

$$W_{j,0} = \epsilon_{i_1 i_2 \cdots i_m} I_{j-(i_1-1)}^{(1)} I_{j-(i_2-1)}^{(2)} \cdots I_{j-(i_m-1)}^{(m)} , \qquad (123)$$

with $\epsilon_{i_1 i_2 \cdots i_m}$ the Levi-Civita symbol. In the above expression, a sum is assumed for each index $i_p = 1, \ldots, m$ ($p = 1, \ldots, m$). Then, with the help of assumption (5), together with Eqs. (95) and (121), we have

$$\begin{aligned}
D_j &= \frac{D_0^{(1)}}{\prod_{\ell=2}^m I_{-\ell}^{(\ell)}} \epsilon_{i_1 i_2 \cdots i_m} I_{j-(i_1-1)}^{(0)} I_{j-(i_2-1)}^{(2)} \cdots I_{j-(i_m-1)}^{(m)} \\
&= \frac{D_0^{(1)}}{\prod_{\ell=2}^m I_{-\ell}^{(\ell)}} W_{j,1} .
\end{aligned} \qquad (124)$$

Substituting now the above expression back into Eq. (119) and recalling the definition of the branch cut amplitude from [11] in terms of d_0 as $\eta(s) := i \, d_0/(2\pi)$, we finally obtain

$$\eta(s) = \Im \left(\frac{1}{\pi W_{-1}^+} \right) \sum_{j=0}^\infty q_j \Xi_{j,1} . \qquad (125)$$

V. REISSNER-NORDSTRÖM SPACETIME

We apply the program presented in the previous sections to the Reissner-Nordström solution. A stationary charged black hole spacetime is characterized by the metric function

$$f(r) = 1 - \frac{2M}{r} + \frac{Q^2}{r^2} = \left(1 - \frac{r_+}{r} \right) \left(1 - \frac{r_-}{r} \right) . \qquad (126)$$

Here M and Q are, respectively, the mass and charge of the black hole, while $r_\pm$ are the coordinate values of the horizons given by

$$r_\pm = M \left[1 \pm \sqrt{1-\epsilon^2} \right], \quad \epsilon = \frac{Q}{M} , \qquad (127)$$

r_+ corresponding to the event horizon and r_- to the Cauchy horizon. The Schwarzschild spacetime is recovered when $\epsilon = 0$, while the extreme black-hole solution is obtained with $\epsilon = 1$. Note that the approach to extremality can lead to different geometries [22, 25].

A convenient alternative parametrization to this spacetime is given in terms of

$$\kappa = \frac{r_-}{r_+} \Rightarrow \epsilon = 2\frac{\sqrt{\kappa}}{1+\kappa} . \qquad (128)$$

The Schwarzschild and extremal black-hole limits correspond to $\kappa = 0$ and $\kappa = 1$, respectively. This new parameter simplifies the expressions we are going to study. In particular, the coordinate locations of the horizons are re-written as

$$r_+ = \frac{2M}{1+\kappa}, \quad r_- = \frac{2M\kappa}{1+\kappa}. \qquad (129)$$

The propagation of scalar, electromagnetic and linear gravitational fields in the Reissner-Nordström spacetime is dictated by the master wave equation (29) introduced in section III A in terms of the potential (cf. [59–62])

$$\mathrm{P}(r) = \ell(\ell+1) + \frac{r_+}{r}\left(\mu - \kappa\, q\, \frac{r_+}{r}\right), \qquad (130)$$

with

$$\mu = \frac{1}{r_+} \times \begin{cases} 2M \\ -3M\left[1 - \sqrt{1 + \epsilon^2\, A}\right] \\ -3M\left[1 + \sqrt{1 + \epsilon^2\, A}\right] \end{cases}$$

$$= \begin{cases} 1 + \kappa \\ -\frac{3}{2}\left[1 + \kappa - \sqrt{(1+\kappa)^2 + 4\kappa A}\right] \\ -\frac{3}{2}\left[1 + \kappa + \sqrt{(1+\kappa)^2 + 4\kappa A}\right] \end{cases}, \qquad (131)$$

$$q = \begin{cases} 2 \\ -4 \\ -4 \end{cases}. \qquad (132)$$

Specifically, the three (ordered) alternative expressions correspond respectively to scalar, electromagnetic and gravitational perturbations. In the expressions above, A stands for $A = \left(\frac{2}{3}\right)^2 (\ell+2)(\ell-1)$.

We are interested, however, in the conformally re-scaled wave equation (45) in section V B, with the potential redefined as (46). For the study of such equation, it will be more convenient to re-parametrize μ and q as

$$\begin{aligned} q &= 3n - 1 \\ \mu &= n(1+\kappa) - (1-n)\mathfrak{m}_\pm \\ \mathfrak{m}_\pm &= \frac{1 + \kappa \pm 3\sqrt{(1+\kappa)^2 + 4\kappa A}}{4}. \end{aligned} \qquad (133)$$

As discussed in section III A 2, the value $n = +1$ for scalar perturbations is a consequence of their natural conformal rescaling. For electromagnetic ($\mathfrak{m}_-$) or gravitational ($\mathfrak{m}_+$) perturbations, the value $n = -1$ is justified in section V B.

A. The hyperboloidal foliation

The hyperboloidal slices are constructed according to the procedure discussed in sections II B and II C. Interestingly, in the context of the minimal gauge, two choices for the conformal representation of the spacetime appear as natural. The first one follows closely the steps in [11, 34, 35, 46] and it consists in fixing the areal radius $\rho(\sigma)$ to a constant — see Eq. (24). The second one maps the Cauchy horizon r_- into a coordinate σ_- that does not depend on the charge parameter κ. As we are going to discuss, the latter provides the geometrical counterpart to the framework introduce by Leaver [29] and it allows us to discuss the near-horizon limit of the extremal black hole.

1. Areal radius fixing

As discussed in section II C 2, the minimal gauge is completely fixed by the free parameters λ and ρ_1. In this section we discuss the first conformal representation case corresponding to fixing the areal radius $\rho(\sigma)$ to a constant value ρ_0. With this aim, and keeping the notation in [11], we choose

$$\lambda = 2r_+, \quad \rho_1 = 0, \qquad (134)$$

which implies $\rho_0 = 1/2$. This choice is equivalent to compactifying the spacetime and defining the height function via

$$r = \frac{r_+}{\sigma}, \quad h(\sigma) = -\frac{1}{\sigma} + (1+\kappa)\ln(\sigma). \qquad (135)$$

As a consequence, the conformal line element reads

$$\begin{aligned} \mathrm{d}\tilde{s}^2 = {}&\frac{1}{4}\,\mathrm{d}\omega^2 - \sigma^2\,(1-\sigma)\,(1-\kappa\sigma)\,\mathrm{d}\tau^2 \\ &+ \left[1 + \sigma(1+\kappa)\right]\left[1 + \kappa(1+\kappa)(1-\sigma)\right]\mathrm{d}\sigma^2 \\ &+ \left(1 - 2\sigma^2\left[1 + \kappa(1+\kappa)(1-\sigma)\right]\right)\mathrm{d}\tau\,\mathrm{d}\sigma \end{aligned} \qquad (136)$$

As prescribed, the event horizon $\mathcal{H}$ is given by $\sigma = 1$ while $\sigma = 0$ locates $\mathscr{I}^+$. Furthermore, the Cauchy horizon r_- is mapped to the value $\sigma_- = \kappa^{-1}$. In particular, we are interested in the exterior region $\sigma \in [0, 1]$.

The transformation (135) and, consequently, the line element (136) is well defined in the whole range of the parameter $\kappa \in [0, 1]$. In particular, the limit $\kappa \to 1$ corresponds to (the standard) extremal Reissner-Nordström (see below and e.g. [23]). However, the algorithm from section IV, based on Taylor expansions, is only valid if $\sigma_- \geq 2$ — see discussion about convergence radius in Eq. (62). Specifically, in this particular coordinate system, methods based on a Taylor expansion around $\sigma = 1$ applies only for $\kappa \in [0, 1/2]$.

2. Cauchy horizon fixing

One way to avoid the limitation imposed in the range of the parameter κ is to fix the location of the Cauchy horizon to a value that does not depend on κ. It is convenient to write σ_- in terms of a constant c, as

$$\sigma_- = c^{-1}. \qquad (137)$$

Together with the choice $\lambda = 2r_+$, this fixes the parameters in the minimal gauge to

$$\rho_0 = \frac{1-\kappa}{2(1-c)}, \quad \rho_1 = \frac{\kappa - c}{2(1-c)}, \qquad (138)$$

which then leads to the compactification and height function

$$r = 2r_+ \frac{\rho(\sigma)}{\sigma} , \quad \rho(\sigma) = \frac{1 - \kappa + \sigma(\kappa - c)}{2(1 - c)} ,$$
$$h = -\frac{1 - \kappa}{\sigma(1 - c)} + (1 + \kappa) \ln \sigma . \quad (139)$$

By fixing the Cauchy horizon at $\sigma_- = c^{-1} > 2$, we ensure that the algorithm based on Taylor expansions around the event horizon $\sigma = 1$ is always valid.

3. Extremality and singular limits

After having introduced the elements of these particular hyperboloidal coordinates, we comment on a geometric aspect relevant in the discussion below, namely the metric type of null infinity, with a focus on the extremal limit.

With this aim, we evaluate the metric type of the vector normal to the hypersurface defined by $\Omega(\sigma) = 0$, with $\Omega(\sigma) = \sigma/\lambda$, as

$$\tilde{\nabla}^a \Omega \tilde{\nabla}_a \Omega = \frac{\sigma^2 F(\sigma)}{\lambda^2 \beta^2}$$
$$= \frac{\sigma^2 (1 - \sigma)(1 - c\sigma)(1 - c)^2}{r_+^2 \left(1 - \kappa + \sigma(\kappa - c)\right)^2} . \quad (140)$$

In the compactification scheme of subsection V A 1, with a gauge enforcing the constancy of the areal radius through $c = \sigma_-^{-1} = \kappa$, one obtains

$$\lim_{\sigma \to 0} \tilde{\nabla}^a \Omega \tilde{\nabla}_a \Omega = 0 , \quad c = \kappa , \quad (141)$$

for all values of κ, including the extremal case $\kappa = 1$. Null infinity is therefore a null hypersurface both in the subextremal and extremal cases, in agreement with the standard extremal limit of Reissner-Nordström. The situation is more delicate for choices $c \neq \kappa$, such as in subsection V A 2. In this case, for $\kappa < 1$ the limit of (140) at $\sigma \to 0$

$$\lim_{\sigma \to 0} \tilde{\nabla}^a \Omega \tilde{\nabla}_a \Omega = 0 , \kappa \in [0, 1) , c \neq \kappa . \quad (142)$$

We find that null infinity for subextremal Reissner-Nordström is a null hypersurface, as obtained in the previous gauge $c = \kappa$. On the other hand, in case of (naively) calculating the limit $\sigma \to 0$ of the expression (140) for $\kappa = 1$ one would get

$$\lim_{\sigma \to 0} \tilde{\nabla}^a \Omega \tilde{\nabla}_a \Omega = r_+^{-2} = M^{-2} , \quad \kappa = 1, c \neq \kappa , \quad (143)$$

suggesting that, in this conformal scheme, the conformal boundary for the extremal case $\kappa = 1$ is timelike [16]. However, we note that the change of coordinates in Eqs. (139) is actually ill-defined for $\kappa = 1$, since the transformation reduces to $r(\sigma) = r_+ = $ constant. This suggests some kind of singular

———

[16] Such timelike null infinity is typical of anti-de Sitter-like (AdS) spacetimes.

behavior in the process of considering the limit of spacetimes as $\kappa \to 1$, when $c \neq \kappa$.

In order to clarify this issue, and since the timelike character of null infinity does not depend on the particular value of c (at least as long as $c \neq \kappa$), let us consider for concreteness the line element of the conformal metric in the gauge of section V A 2 defined by transformations (139). In addition, we choose for simplicity $c = 0$ or, equivalently, $\sigma_- \to \infty$. Then

$$d\tilde{s}^2 = \frac{1 - \kappa}{4\rho^2} \Bigg(-(1 - \kappa) \sigma^2 (1 - \sigma) d\tau^2$$
$$- \left(1 - 2\sigma^2 - 2\kappa(1 - \sigma) [(2 - \kappa(1 - \sigma)] \right) d\tau d\sigma$$
$$+ [1 + \sigma - \kappa(1 - \sigma)] d\sigma^2 \Bigg) + \rho^2 d\omega^2 . \quad (144)$$

The pathological behavior for $\kappa = 1$ in this gauge is apparent in the line element. However, a regularization is obtained through the introduction of an appropriate re-scaling of the time coordinate

$$T = (1 - \kappa)\tau . \quad (145)$$

The combined transformations (139) and (145), for $\kappa < 1$, lead to [25]

$$d\tilde{s}^2 = \frac{1}{4\rho^2} \Bigg(-\sigma^2 (1 - \sigma) dT^2$$
$$- \left(1 - 2\sigma^2 - 2\kappa(1 - \sigma) [(2 - \kappa(1 - \sigma)] \right) d\tau d\sigma$$
$$+ (1 - \kappa) [1 + \sigma - \kappa(1 - \sigma)] d\sigma^2 \Bigg) + \rho^2 d\omega^2 \quad (146)$$

This expression makes now also sense in the limit $\kappa \to 1$, defining the line element

$$d\tilde{s}_{\text{ext}}^2 = -(1 - \sigma) dT^2 + dT d\sigma + \sigma^2 d\omega^2 . \quad (147)$$

The corresponding physical manifold $ds^2 = \Omega^{-2} d\tilde{s}^2$, called the Bertotti-Robinson metric, is the near-horizon limit of the extremal black hole. Its topology is a direct product of $1 + 1$ AdS spacetime with a sphere of constant radius, indeed with a timelike null infinite in accordance with the expression in (143). We are therefore in the presence of two different extremal limits of Reissner-Nordström, an illustration of the subtleties to be considered when discussing the limits of spacetimes [21, 22].

4. Geometric insights into Leaver's treatment

The previous discussion on singular limits of spacetimes is not academical. On the contrary, it is directly relevant to Leaver's treatment of QNMs in Reissner-Nordström [29] since, as we show below, the latter corresponds to the gauge choice in subsection V A 2, namely the fixing of the Cauchy horizon coordinate position with $\sigma_- = \infty$. Since, as seen in

V A 3, such coordinates suffer a singular extremal limit, the question is raised about the QNM calculation following [29] in the extremal limit.

Let us justify the connection between Leaver's treatment in [29] and the coordinates introduced in V A 2. For this, let us consider the coordinate u in the Taylor expansion (61), a coordinate that naturally emerges in the geometric discussion in terms of hyperboloidal slices. Indeed, under the choice $c = 0$ leading to the line element (144) and fixing the Cauchy horizon at $\sigma_- = \infty$, such coordinate u is written in terms of the original coordinate r as

$$u = \frac{r - r_+}{r - r_-} \, . \tag{148}$$

This is precisely the coordinate introduced by [29], here identified within a natural geometric setting. The key point in the present discussion refers to the fact that the treatment in [29] (based on Cauchy slices) requires the introduction of regularization factors in the Taylor expansion in order to deal with the QNM asymptotic conditions. Remarkably, and as it happened in [11], such factors arise in the present discussion directly as a consequence of the geometric treatment in terms of hyperboloidal slices. As a matter of fact, the factor Z in Eq. (55) reads

$$\begin{aligned} Z(r) &= \rho^n e^{s\left[\frac{r^*}{\lambda} + h\right]} \\ &= C\rho^n \left(\frac{r_+}{r}\right)^{s_\kappa} e^{-s_\kappa r_\kappa} \left(1 - \kappa\frac{r_+}{r}\right)^{-s_\kappa} u^b \, , \end{aligned} \tag{149}$$

where C is a constant. The parameters

$$s_\kappa = \frac{(1 + \kappa)s}{2}, \ r_\kappa = \frac{r}{(1 + \kappa)r_+}, \ b = \frac{s}{2(1 - \kappa)} \, , \tag{150}$$

are adapted to the normalization used in [29].

For $n = -1$, the factors in (149) coincide exactly with the ones appearing multiplying the Taylor expansion in [29]. More specifically, the first factor (an appropriate power of ρ) was introduced in [29] to reduce the number of terms in the recurrence relation — see section V B — whereas the rest were introduced to incorporate the boundary conditions appropriate for QNMs.

In contrast, in the present discussion the factor ρ^n is motivated as a direct consequence of using the *conformal* wave equation, whereas the rest of the factors are a straightforward consequence of the use of hyperboloidal slices.

Note that [29] considers only electromagnetic and gravitational perturbations. Therefore we are led to the conclusion that the appropriate conformal re-scaling factor introduced in section III A 2 is $n = +1$ for scalar field and $n = -1$ for electromagnetic and linear gravitational fields

To summarize the discussion in this section V A, we identify two relevant outcomes of the present geometric approach:

(i) It is the simultaneous combination of a conformal approach and the use of the hyperboloidal slices that renders a geometric explanation of the factors in Leaver's Taylor expansion approach to QNMs.

(ii) Such geometric perspective provides an insight into the extremal limit corresponding to Leaver's QNM calculation. Indeed, according to the discussion above, the approach to extremality in [29] (i.e. $c = 0$) would correspond to the Bertotti-Robinson spacetime rather than the standard extremal Reissner-Nordström. A natural question to assess is the relation between the limit values of QNMs in such approach to $\kappa \to 1$ and the QNMs directly calculated in the standard extremal Reissner-Nordström spacetime [63].

B. Laplace analysis

We now proceed to write explicitly all the elements for the Laplace analysis of the Reissner-Nordström spacetime in the hyperboloidal minimal gauge. We consider here the two cases discussed in the previous section, namely V A 1 and V A 2.

1. Areal radius fixing

Here, the areal radius is fixed to $\rho_0 = 1/2$ and the Cauchy horizon depends on the charge parameter as $\sigma_- = \kappa^{-1}$. According to the discussion in section III A, in this particular gauge there is no distinction between considering a wave equation based on a conformally invariant framework (45) or simply applying a coordinate transformation into the well-known formulation (29).

The Laplace operator (49) and the source function (50) read

$$\begin{aligned} \mathbf{A}(s) = {}& \sigma^2 (1 - \kappa\sigma)(1 - \sigma)\partial_{\sigma\sigma} + \bigg((2 - 3\sigma)\sigma \\ &+ \kappa\sigma^2(4\sigma - 3) + s\left[1 - 2\sigma^2 - 2\kappa(1 + \kappa)\sigma^2(1 - \sigma)\right]\bigg)\partial_\sigma \\ &- \bigg(\ell(\ell + 1) + \sigma(\mu - \kappa q\sigma) + s\sigma\left[2 + (2 - 3\sigma)\kappa(1 + \kappa)\right] \\ &+ \left[1 + (1 - \sigma)\kappa(1 + \kappa)\right]\left[1 + \sigma(1 + \kappa)\right]s^2\bigg), \end{aligned} \tag{151}$$

$$\begin{aligned} B(s) = {}& -\left[1 + (1 - \sigma)\kappa(1 + \kappa)\right]\left[1 + \sigma(1 + \kappa)\right]\left(s\Phi_0 + \dot\Phi_0\right) \\ &+ \bigg(1 - 2\sigma^2\left[1 + \kappa(1 + \kappa)(1 - \sigma)\right]\bigg)\Phi_{0,\sigma} \\ &- \sigma\left[2 + (2 - 3\sigma)\kappa(1 + \kappa)\right]\Phi_0 \, . \end{aligned} \tag{152}$$

With the expansion around the horizon (61), we obtain a 3-order recurrence relation. According to our notation — see

Eqs. (63) and (75) — we have $m = 2$ and coefficients

$$\alpha_k = (k+1)\left[s + (1-\kappa)(1+k)\right],$$

$$\begin{aligned}\beta_k^{(0)} &= -\ell(\ell+1) - \mu - 2(k+s+1)(k+s) + s\kappa^2(1+2k)\\ &\quad +\kappa\left[(k+s)(3k-s+1) + q + 2k\right]\end{aligned} \tag{153}$$

$$\begin{aligned}\beta_k^{(1)} &= \mu - 1 + (k+s)^2 - \left[(k+s)(s+3k) + 2q - 3\right]\kappa\\ &\quad -(s\kappa + 4k + 3s)s\kappa^2\end{aligned}$$

$$\beta_k^{(2)} = \kappa\left(\kappa s + k + s + 1\right)\left(\kappa s + k + s - 2\right) + \kappa q .$$

A study of the asymptotic behavior of the solutions to the homogeneous recurrence relation shows — cf. the discussion around (68).

$$I_k^{(0)} \sim e^{\xi\sqrt{k}}k^\zeta, \ \ I_k^{(1)} \sim e^{-\xi\sqrt{k}}k^\zeta, \ \ I_k^{(2)} \sim v^k k^\varsigma , \tag{154}$$

with

$$\xi = 2\sqrt{s}, \quad v = \frac{\kappa}{\kappa - 1} , \tag{155}$$

$$\zeta = \frac{1+\kappa}{2}s - \frac{3}{4}, \quad \varsigma = -\left(1 + \frac{\kappa^2}{1-\kappa}s\right) . \tag{156}$$

As expected, assumption (2) in section IV A is valid only for $\kappa \in [0, 1/2]$. Indeed, for $\kappa > 1/2$, $I_k^{(2)}$ is no longer a decaying solution and its growth reflects the fact that the Cauchy horizon $\sigma_- = \kappa^{-1} < 2$ has entered the unit circle (62).

2. Cauchy horizon fixing

In this case, the Cauchy horizon is fixed at $\sigma_- = \infty$ and the areal radius reads

$$\rho(\sigma) = \frac{1 - \kappa(1-\sigma)}{2} .$$

Since $\rho(\sigma)$ is no longer a constant, Eqs. (33) and (45) differ in this gauge. As stated previously, from the theoretical perspective, we regard the conformally invariant wave equation as the most natural choice, due to its geometrical formulation. Thus, the Laplace operator (49) reads[17]

$$\begin{aligned}\mathbf{A}(s) &= (1-\kappa)\sigma^2(1-\sigma)\partial_{\sigma\sigma} + \Bigg(\sigma\left[2 - \sigma(1+2n)\right]\\ &\quad -\frac{(1-n)\sigma^2}{\rho} - 2s(\sigma^2 - 2\rho^2)\Bigg)\partial_\sigma - s^2(\sigma + 2\rho)\\ &\quad -2s\left[\sigma - \kappa\rho n - \frac{\kappa(1-n)\sigma^2}{2\rho}\right] - (1-\kappa)\Bigg(\ell(\ell+1)\\ &\quad +\sigma + (1-n)\left[1 - \frac{1-\kappa+\sigma(1+\mathfrak{m}_\pm)}{2\rho}\right]\Bigg) , \end{aligned} \tag{157}$$

---

[17] In the Cauchy fixing gauge, expressing explicitly the dependence of the parameter m and q in terms of n — cf. (133) — simplifies the form of the operator $\mathbf{A}(s)$. This accounts for the appearance of parameters n and $\mathfrak{m}_\pm$ in Eq. (157). In particular, terms going as ρ^{-1} vanish for $n = 1$.

with the source given by

$$\begin{aligned}B(s) &= -(\sigma + 2\rho)\left(s\Phi_0 + \dot{\Phi}_0\right) - 2(\sigma^2 - 2\rho^2)\Phi_{0,\sigma}\\ &\quad -2\left[\sigma - \kappa\rho n - \frac{\kappa(1-n)\sigma^2}{2\rho}\right]\Phi_0 . \end{aligned} \tag{158}$$

The choice of Eq. (45) (instead of (33)) is also justified from a practical point of view, as the Taylor expansion (61) leads to a simpler recurrence relation. Indeed, the recurrence relation for scalar perturbations is actually of order 2 ($m = 1$) with coefficients

$$\begin{aligned}\alpha_k &= (k+1)\left[s + (1-\kappa)(1+k)\right]\\ \beta_k^{(0)} &= -(1-\kappa)\left[1 + \ell(\ell+1) + 2k(k+s+1)\right]\\ &\quad +s\left[\kappa - 2(k+s+1)\right]\\ \beta_k^{(1)} &= \left[k + s(1+\kappa)\right]\left[s + k(1-\kappa)\right] . \end{aligned} \tag{159}$$

The asymptotic behaviors for the solutions of the homogeneous recurrence relation are

$$I_k^{(0)} \sim e^{\xi\sqrt{k(1-\kappa)}}k^\zeta, \ \ I_k^{(1)} \sim e^{-\xi\sqrt{k(1-\kappa)}}k^\zeta , \tag{160}$$

with ξ and ζ still given by (155) and (156).

For electromagnetic/gravitational perturbations ($n = -1$), we obtain the 3-order recurrence relation ($m = 2$)

$$\begin{aligned}\alpha_k &= (k+1)\left[s + (1-\kappa)(1+k)\right]\\ \beta_k^{(0)} &= -(1-\kappa)\left[\ell(\ell+1) + \mu\right] - 2(k+s+1)\left[s + k(1-\kappa)\right]\\ &\quad +\kappa(k-3)\left[(1-k)(1-\kappa) - s\right]\\ \beta_k^{(1)} &= \left[-1 + \mu + \kappa\ell(\ell+1) + 12\kappa\right](1-\kappa)\\ &\quad +(k+s)^2(1+\kappa) + 2\kappa(s-5)\left[k + s(1-\kappa)\right]\\ &\quad -(k+2s-5)(2k-s)\kappa^2\\ \beta_k^{(2)} &= -\kappa\left[s(1+\kappa) + k - 3\right]\left[s + (k-3)(1-\kappa)\right] . \end{aligned} \tag{161}$$

Apart from (160), there exists here a third solution to the homogeneous recurrence relation whose asymptotic behavior is

$$I_k^{(2)} \sim \kappa^k k^{-6} . \tag{162}$$

C. Results

We end this section with the application of the algorithm from section IV to the Reissner-Nordström spacetime. As a representative example, we show here results for scalar and gravitational fields, whereas the discussion in Appendix VII B is exemplified by an electromagnetic perturbation. The qualitative discussion, though, does not depend on the specific choice of the parameters in the effective potential.

We first calculate the QNM frequencies as the zeros of the Wronskian determinant W_{-1} (95). The algorithm for this procedure is described in [11] (cf. section IV.D.2 in that reference). The results were obtained by dividing the interval $\kappa = [0, 0.5]$ (areal radius fixing gauge) or $\kappa = [0, 0.99]$ (Cauchy horizon fixing gauge) into an equidistant κ-grid of size $\sim 10^{-2} - 10^{-3}$.
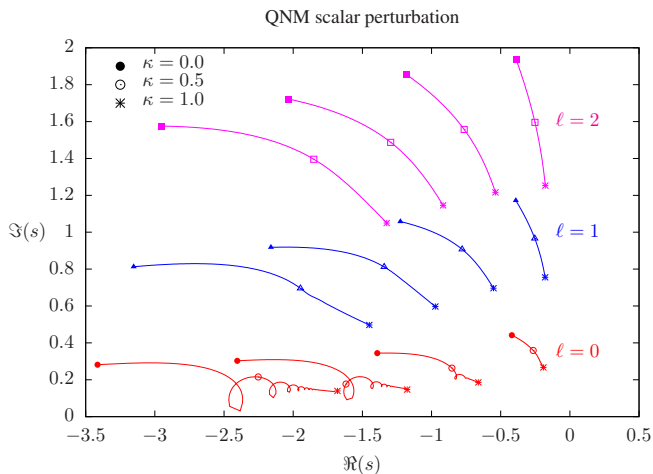
Fig. 3 displays the results for scalar perturbations with $\ell = 0$ (red circle), $\ell = 1$ (blue triangle) and $\ell = 2$ (magenta square). The solid points are the values for the Schwarzschild solution $\kappa = 0$, whereas the empty points mark the value $\kappa = 0.5$ for which the specific algorithm from section IV ceases to be valid in the "areal radius fixing" gauge. As expected, the results for $\kappa \in [0, 0.5]$ coincide in both gauges. Moreover, in the "Cauchy horizon fixing" gauge we can calculate further until $\kappa \lesssim 1$. The value $\kappa = 1$ is not available in this gauge because the limiting process is discontinuous and it leads to the near-horizon geometry. It is interesting to notice that the looping structure in the higher QNMs for the scalar field with angular mode $\ell = 0$ is not an artifact of the numerical resolution, but it actually reflects the parametric dependence of the QNMs on κ[18].

QNM scalar perturbation

FIG. 3. Quasi-normal modes for scalar perturbations for $\ell = 0$ (red circle), $\ell = 1$ (blue triangle) and $\ell = 2$ (magenta square). The solution was obtained in the "areal radius fixing" gauge ($\kappa \in [0, 0.5]$) and the "Cauchy horizon fixing" gauge ($\kappa \in [0, 0.99]$). The Schwarzschild value ($\kappa = 0$) is given by solid points, while the empty points mark the limit of validity for the method in the "areal radius fixing" gauge ($\kappa = 0.5$). Even though the extremal limit in the "Cauchy horizon fixing" gauge leads to the Robinson-Bertotti spacetime, a continuous extrapolation from the values for $\kappa \lesssim 1$ into the extremal value $\kappa = 1$ is consistent with the results obtained in literature [63] (star points).

The limitation in the calculation of the QNMs in the "areal radius fixing" gauge for $\kappa \leq 0.5$ is a consequence of the method — see discussion around Eq. (62) — and not an intrinsic issue of QNMs. Other methods — such as the one[19] employed in [15] — can be used to calculate the modes in the full range $\kappa \in [0, 1]$. In particular, this alternative method was used, on the one hand, to confirm the looping structure in the

---

[18] We do not have an explanation for this behavior and a clarification would require further work.

[19] The work [15] describes an alternative method to calculate not only the QNMs, but also the discrete amplitudes η_n. The method, however does not allow us to calculate the branch cut amplitude $\eta(s)$.
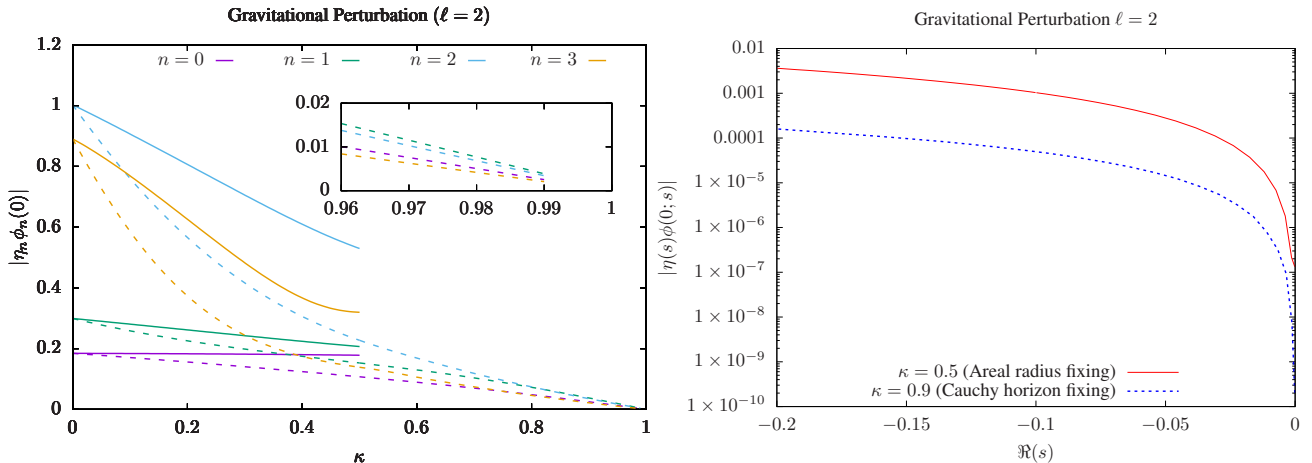
higher QNMs for the scalar field with angular mode $\ell = 0$. On the other hand, the method from [15] allows us to calculate the QNMs for the extremal Reissner-Nordström case $\kappa = 1$ (star points in Fig. 3).

The results are in accordance with the literature [63] and they are consistent with a continuous extrapolation of the values obtained in the "Cauchy horizon fixing" gauge. This allows us to answer the question posed in point (ii) at the end of section V A 4: the discontinuous spacetime limit at $\kappa \to 1$ does not reflect in a discontinuous limit in the QNMs. This naturally raises the issue of a possible "QNM-isospectrality" between extremal Reissner-Nordström and the near-horizon Bertotti-Robinson metric.

Once QNM frequencies are obtained, we address the resonant expansion aspects of the algorithm. That is, we proceed to the calculation of the amplitudes η_n related to each QNM and to the branch cut $\eta(s)$ for given initial data. As a representative example, we consider a gravitational perturbation with angular mode $\ell = 2$ and the initial data

$$V_0(\sigma) = \sigma(1 - \sigma) \quad \dot{V}_0(\sigma) = 0 . \tag{163}$$

In particular, we show in Fig. 4 the invariants $\eta_n \phi_n(\sigma)$ and $\eta(s)\phi(s;\sigma)$, both calculated at $\mathscr{I}^+$ (i.e. $\sigma = 0$).

The left panel shows the dependence of the QNM amplitude η_n as a function of κ for the "areal radius fixing" gauge for $\kappa \in [0, 0.5]$ (solid lines) and the "Cauchy horizon fixing" gauge $\kappa \in [0, 0.99]$ (dashed lines). In particular, the inset displays the value around $\kappa \lesssim 1$ where we observe a tendency towards zero. A full understanding of this limiting behavior would require the control of boundary data. Indeed, since the limiting spacetime in the "Cauchy horizon fixing" gauge has a timelike boundary involving the geometry of AdS$_2$, a unique solution to the wave equation is no longer obtained only with the initial data (163), since boundary conditions at $\sigma = 0$ are required as well. In [15], the QNM amplitudes of asymptotically AdS spacetimes are obtained after reformulating the corresponding wave equations to include the Dirichlet boundary conditions.

The right panel of Fig. 4 shows $|\eta(s)\phi(s;\sigma)|$ around $s = 0$ for $\kappa = 0.5$ ("areal radius fixing" gauge) and $\kappa = 0.9$ ("Cauchy horizon fixing" gauge). The behavior of the branch cut amplitude around the origin is responsible for the late-time tail decay. Indeed, assuming that

$$\eta(s)\phi(s;\sigma) \sim s^\gamma , \tag{164}$$

we obtain

$$V_{\text{tail}}(\tau, \sigma) = \int_{-\infty}^0 \eta(s)\phi(s;\sigma)e^{s\tau}ds$$

$$\sim \int_{-\infty}^0 s^\gamma e^{s\tau}ds \sim \tau^{-(\gamma+1)} . \tag{165}$$

From the plot in Fig. 4, one can read the behavior $\gamma = 2$, which should lead to the expected tail decay τ^{-3} along future null infinity [7]. Indeed, Fig. 5 shows the complete time dependence according to the spectral decomposition (2) for $\kappa = 0.5$ ("areal radius fixing" gauge) and $\kappa = 0.9$ ("Cauchy

FIG. 4. Left panel: quasi-normal mode amplitudes $\eta_n\phi_n(\sigma)$ at $\sigma = 0$ as functions of the charge parameter κ for the first four quasi-normal modes. The solid lines display the results in the "areal radius fixing" gauge ($\kappa \in [0, 0.5]$), while the dashed lines correspond to the "Cauchy horizon fixing" gauge ($\kappa \in [0, 0.99]$). The inset focuses on the behavior around $\kappa = 1$ and it shows that the amplitudes vanish in the limit to the Robinson-Bertotti spacetime. Right panel: branch cut amplitudes at $\sigma = 0$ for $\kappa = 0.5$ ("areal radius fixing" gauge) and $\kappa = 0.9$ ("Cauchy horizon fixing" gauge). Both behave as s^2, leading to a late time decay in the form τ^{-3} — see Fig. 5.

horizon fixing" gauge). Specifically, we have considered only the first 4 dominant QNMs in the spectral decomposition (2). Moreover, the integration along the branch cut is performed here just in the interval $s \in [-0.2, 0)$ which is enough to focus on the late times. For comparison, the figure also brings the evolution obtained via an explicit time integration of the wave equation with the code [46], the inset displaying the match between both methods for $\tau \sim 0$. Notice the remarkable agreement between the spectral decomposition (2) and the time evolution — see last paragraph in appendix VII A for a discussion concerning the assessment of conjecture 1.

VI. DISCUSSION

In this article we have studied the spectral decomposition of solutions to dissipative linear wave equations formulated on spherically symmetric, stationary and asymptotically flat spacetimes containing a black hole. Focus has been placed on a particular geometric frame that exploits the use of conformal compactifications together with a foliation in hyperboloidal hypersurfaces. Specifically, we extend the results in [11] by (i) defining the so-called minimal gauge, as the simplest hyperboloidal gauge adapted to a spherically symmetric, stationary and asymptotically flat, black-hole spacetime and by (ii) generalizing the semi-analytical algorithm based on a Taylor expansion that enables us to construct the ingredients $\{s_n, \phi_n, \eta_n\}_{n=1}^{\infty}$ as well as $\{\phi(s), \eta(s)\}_{s \in \mathbb{R}^-}$ of the spectral decomposition (2). Such extensions involve non-trivial technical generalizations allowing us now to deal with multiple horizon settings and higher-order recurrence relations in the underlying algorithm. Moreover, we have detailed the discussion on how this geometrical framework gives rise naturally to the regularization factors needed in the usual Cauchy-based foliation to incorporate the appropriate boundary conditions

leading to QNMs.

As a particular example, we have applied the formalism to the Reissner-Nordström spacetime. In a first stage we have focused on the geometric content of the framework, showing that the minimal gauge leads to two natural different conformal hyperboloidal compactifications, referred in this paper as "areal radial fixing" and "Cauchy horizon fixing". The former fixes the areal radius of the conformal spacetime ρ to a given constant value, leading to a system in which the coordinate value of the Cauchy horizon depends on the charge parame-
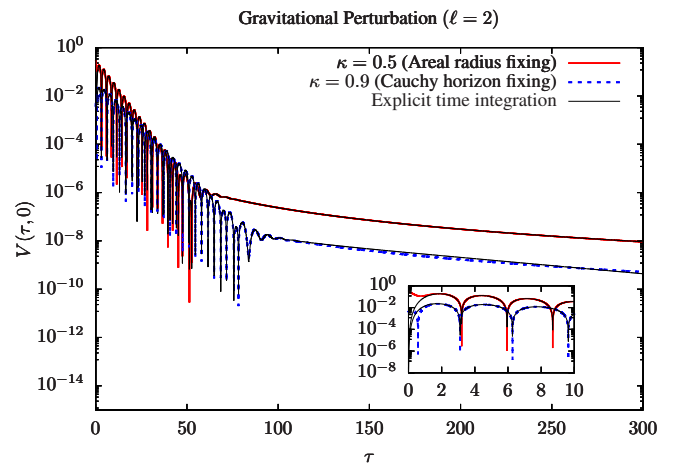

FIG. 5. Time dependence according to the spectral decomposition (2). The solid red line is obtained for $\kappa = 0.5$ in the "areal radius fixing" gauge, whereas the dashed blue line is for $\kappa = 0.9$ in the "Cauchy horizon fixing" gauge. The black solid line corresponds to the explicit time evolution with the code [46]. The inset focus on the match between both methods around $\tau = 0$.

ter κ. The latter, instead, fixes the coordinate location of the Cauchy horizon to a value independent of the charge parameter.

While both gauges reduce in the Schwarzschild limit $\kappa = 0$ to the coordinate system used in [11], they lead to different geometries in the limit to extremality. For $\kappa = 1$, the "areal radial fixing" gauge provides the usual extremal Reissner-Nordström black-hole limit, while the "Cauchy horizon fixing" gauge has the near-horizon geometry as limit. This solution — the so-called Bertotti-Robinson spacetime — is the direct product of AdS_2 with a sphere of constant radius. Even though the distinct spacetime limits were previously discussed in [24, 25], they were recovered in this work via different choices for the conformal compactification of the spacetime. It would be insightful to study the topic of spacetime limits in a more generic context within the realm of conformal methods in General Relativity [64].

On the top of that, we have also identified the "Cauchy horizon fixing" gauge as the geometrical counterpart to Leaver's treatment of QNMs in Reissner-Nordström [29]. It is well-known that Leaver's methodology is not valid at $\kappa = 1$ (cf. e.g. [29, 63]). Due to the understanding of the limiting process in the "Cauchy horizon fixing" gauge, we conclude that the limitation in Leaver's algorithm is not just technical, but rather a consequence of the geometry involved.

Note that the original algorithm [29] was modified in [63] to treat the extremal case exclusively. The strategy[20] was to perform the Taylor expansion around the point $r_0 = r_+/2$ instead of $r_0 = r_+$. Even though the conclusion is that "the numerically computed values are consistent with the values earlier obtained by Leaver", we would like to stress that the comparison between both works is not as straightforward as expected. Indeed, from the geometrical point of view, the spacetime studied in Onazawa et. al [63] corresponds to the extremal limit achieved within the "areal radial fixing" gauge. Leaver's approach — being based on the "Cauchy horizon fixing" gauge — has a discontinuous limit to extremality into the Bertotti-Robinson spacetime.

An interesting open question is to determine whether such Bertotti-Robinson spacetime admits some natural conditions in the AdS boundary leading to the same QNMs as the ones in the usual extremal limit. The assessment of such QNM-isospectrality between extremal Reissner-Nordström and the corresponding near-horizon geometry could offer insight into correlations between geometrical properties at the horizon and at null infinity [66–69] in extremal black hole settings.

In a second stage, we have applied the algorithm developed in section IV to construct the solution — in general, after an initial transitory — to the dissipative wave equation in terms of the spectral decomposition (2). In this context, the "areal radial fixing" gauge has a technical limitation. Since the coordinate value of the Cauchy horizon depends on the charge parameter κ, the convergence radius of the Taylor expansion reduces as the Cauchy horizon approaches the event horizon.

In particular, the algorithm is valid for the values $\kappa \in [0, 1/2]$. Working in the "Cauchy horizon fixing" gauge is a natural first solution to this limitation. As already mentioned, however, this option changes the geometry of the limiting extremal spacetime.

An alternative solution would be to follow [63, 65] and adapt the algorithm to a Taylor expansion around $r_0 = r_+/2$ for *all* values of κ (and not only to the extremal case). In our compactified radial coordinate, this corresponds to an expansion around the regular point $\sigma_0 = 1/2$. In this case, assumption (I) in section IV A is not valid anymore as one obtains, in fact, two independent solutions satisfying Eq. (71). The exploration of this particular possibility requires a specifically dedicated study.

We conclude by pointing out that the geometrical framework and/or the semi-analytical algorithm developed here are promising and potentially valuable tools in several fields. In the new era of gravitational wave astronomy, we intend to further explore the extraction of highly-accurate waveforms for binary black-hole systems in the large-mass-ratio regime [70–76], apart from studying models extending beyond General Relativity [77, 78]. On the other hand, resonant expansions in optical systems have proved to be an efficient tool in the study of the near-field properties of nano-resonators [8]. The algorithm developed here, conveniently adapted to the dispersive case with a frequency-dependent permittivity, could shed light into the ambiguities in the determination of the QNM expansion coefficients in such optical setting [21]. Finally, on a purely mathematical ground, the issues here raised in the calculation of QNMs in singular spacetime limits define a non-trivial problem on "resonance isospectrality" in the setting of the spectral analysis of non-selfadjoint operators[79].

---

[20] The same strategy was recently used in the context of the extremal Kerr black hole [65] as well.

---

[21] In the optical context tails play typically no role in the spectral expansion (2), due to the compact support of the domain in which the spatial dependence of the permittivity deviates from its background (constant) value. In this sense, the optical case simplifies with respect to the gravitational one.

VII. APPENDIX

A. Spectral elements and resonant asymptotic expansions

We sketch here briefly the basic spectral elements needed to characterize QNMs, with a focus on the notion of resonant expansion, in an attempt of better seizing conjecture 1.

Let us consider the wave equation in $\mathbb{R} \times \mathbb{R}^n$, with n odd

$$
\begin{cases}
\left(\partial_t^2 - \Delta + V(\mathbf{x})\right) \Phi(t, \mathbf{x}) = 0 \,, \\
\Phi(0, \mathbf{x}) = \Phi_0(\mathbf{x}) \,, \\
\partial_t \Phi(0, \mathbf{x}) = \Phi_1(\mathbf{x}) \,,
\end{cases}
\tag{166}
$$

with Δ the Laplacian in $\mathbb{R}^n$, $V(\mathbf{x})$ a bounded potential and $\Phi_0(\mathbf{x})$ and $\Phi_1(\mathbf{x})$ prescribed initial data[22]. Defining the elliptic operator in $\mathbb{R}^n$

$$
P_V = -\Delta + V \,,
\tag{167}
$$

Eq. (166) becomes, under Laplace transformation

$$
\left(P_V + s^2\right) \hat{\Phi}(s, \mathbf{x}) = S(s, \mathbf{x}) \,,
\tag{168}
$$

with $S(s, \mathbf{x})$ a source defined in terms of the initial data, as $S(s, \mathbf{x}) = s\Phi_0(\mathbf{x}) + \Phi_1(\mathbf{x})$.

A key element in the spectral analysis of Eq. (166) is provided by the notion of the resolvent $R_V(s)$ of P_V. Such operator is defined, between the appropriate domain and codomain functional spaces, as the inverse of the operator on the left-hand-side of Eq. (168), that is[23]

$$
R_V(s) = \left(P_V + s^2 \, \mathrm{Id}\right)^{-1} \,.
\tag{170}
$$

For appropriate potentials V, the resolvent can be shown to be analytical in the right half-plane $\Re(s) > 0$ of the complex spectral parameter. Then, under the suitable assumptions on V, a meromorphic extension of $R_V(s)$ exists in the left half-plane $\Re(s) < 0$. Scattering resonances, i.e. QNMs frequencies s_n, are then defined as poles in such meromorphic extension. For potentials V not decaying sufficiently fast at infinity, the extension of $R_V(s)$ to the whole s-complex plane presents a more complicated analytical structure. In particular, as commented in footnote 1, in the Schwarzschild case a branch cut starting at $s = 0$ appears in addition to the QNM poles, giving rise to a tail contribution at late times. This is also the case

---

[22] Assumptions on the initial data functional spaces are required, e.g. $\Phi_0(\mathbf{x}) \in H^1(D)$ and $\Phi_1(\mathbf{x}) \in L^2(D)$, with D an appropriate domain $D \subset \mathbb{R}^n$.

[23] The resolvent $R_V(s)$ is intimately related to the Green function $G_s(\mathbf{x}-\mathbf{y})$ of $\left(P_V + s^2\right)$, characterized as $\left(P_V + s^2\right) G_s(\mathbf{x}-\mathbf{y}) = \delta^{(n)}(\mathbf{x}-\mathbf{y})$, so that the Green function is the integral kernel of the resolvent operator

$$
R_V(s)(\Phi)(\mathbf{x}) = \int_{\mathbb{R}^n} G_\omega(\mathbf{x}-\mathbf{y}) \Phi(\mathbf{y}) d^n \mathbf{y} \,.
\tag{169}
$$

The resolvent of P_V is usually defined as $R_V(\lambda) = (P_V - \lambda \, \mathrm{Id})^{-1}$, with λ as *spectral parameter*. In the present scattering context, one takes $\lambda = \omega^2$ as spectral parameter, with ω the Fourier parameter in Eq. (1). Finally, the discussion in terms of the Laplace transform (cf. e.g. section I), with parameter $s = i\omega$, leads to the version (170) of the resolvent.

---

in the here studied Reissner-Nordström (cf. [9, 10] and references therein for a spectral analysis discussion of scattering resonances, as well as [80] for a more heuristic account, in particular addressing tails and initial transient issues).

The elements introduced above allow us to address a central point in this work, namely conjecture 1 concerning the spectral decomposition (2) of the scattered field. A claim on QNM *completeness* (together with tail functions) would require: (i) the identification of some appropriate functional space for the scattered fields, and (ii) a claim on the convergence of the series in (2) in such linear space. No claim is made here in this respect. It is known that QNM completeness is a property of very particular potentials (cf. e.g. [81] where QNM completeness is shown for a Pöschl-Teller potential) and does not hold in general. On the other hand, for suitable potentials, sound results hold for resonant or QNM expansions, if understood as *asymptotic expansions*. It is in this sense that, in principle, the series in (2) must be interpreted.

To illustrate this point on asymptotic expansions, we refer to the results on resonant expansions of scattered waves by Lax and Phillips [82] and Vainberg [83]. For concreteness, for bounded potentials V under the appropriate hypotheses (namely on their support) the following kind of result can be shown (cf. e.g. [9, 10] for full details and background): for any $a > 0$ the scattered field solution to Eq. (166) can be written as a 'resonant expansion' in terms of QNMs

$$
\Phi(t, \mathbf{x}) = \sum_{\Re(s_j) > -a} u_j(\mathbf{x}) e^{s_j t} + E_a(t) \,,
\tag{171}
$$

where $\{s_j\}_{j=1}^{\infty}$ are the resonances of P_V —namely the poles of the meromorphic extension of $R_V(s)$, as discussed above— and u_j are the corresponding resonant states, determined also in terms of the resolvent $R_V(s)$ as[24]

$$
u_j = i \, \mathrm{Res}_{s=s_j} \left(R_V(s)\Phi_1 + s R_V(s)\Phi_0\right) \,.
\tag{172}
$$

The QNM sum in (171) is finite if the resonant frequencies s_n do not accumulate near the imaginary axis and, crucially for our discussion on asymptotic series, constants C_a and T_a exist such that the error $E_a(\tau)$ can be bound for $\tau \geq T_a$ as

$$
\|E_a(t)\|_{H^1} \leq C_a e^{-a\tau} \left(\|\Phi_0\|_{H^1} + \|\Phi_1\|_{L^2}\right) \,, \ \tau \geq T_a \,.
\tag{173}
$$

The key point we want to stress here is that the bound (173) on the error $E_a(\tau)$ is *not uniform* in a. This means that we can indeed incorporate more QNMs into the resonant expansion by enlarging the "band" in the left half-complex plane defined by each *fixed* a, but nothing guarantees that the constant C_a does not explode in the process. As a consequence, in general actual convergence cannot be shown and we must treat the QNM expansion rather as an asymptotic series.

---

[24] Note that the resonant state $u_j(\mathbf{x})$ is obtained through the application of the resolvent $R_V(s)$ on the source $S(s, \mathbf{x})$ in (168), consistently with its link with the Green function. Note, comparing (2) and (171) that the 'meaningful' quantity is indeed the combination $u_j = \eta_j \phi_j$, and not η_j and ϕ_j separately. This justifies the term *invariant* for the amplitudes in Fig. 4.

Once we have insisted in the, a priori, asymptotic character of the QNM expansion in conjecture 1, let us bring attention to the remarkable result shown in Fig. 5: the extraordinary agreement —at all time scales— between the explicit time evolution of the initial data and its 'spectral expansion' (2) poses the prospect of an actual 'full' convergence in some appropriate space and, therefore, QNM and tail completeness in the Reissner-Nordström case. Such a possibility should be studied with tools different from the ones in the present work.

B. Backward recurrence relation

A key element in the algorithm from [11] when constructing the decaying solutions in assumption (2) is the usage of a *backward* iteration of the homogeneous Eq. (63). Here, we review how to construct the decaying solutions with such a technique in the present context and discuss the instability issues arising from the backward iteration.

According to the algorithm from section IV A, inserting the Ansatz (68) back into the recurrence relation (63) and multiplying the result by $e^{-\xi k^p} k^{-\zeta}$, leads to

$$
0 = \alpha_k e^{-\xi k^p[1-(1+k^{-1})^p]}(1+k^{-1})^\zeta A_{k+1}
$$
$$
+ \sum_{i=0}^{m} \beta_k^{(i)} e^{-\xi k^p[1-(1+ik^{-1})^p]}(1-ik^{-1})^\zeta A_{k-i} . \quad (174)
$$

For a fixed asymptotic parameter p, we expand the above expression in terms of $y = k^{-p}$ around $y = 0$, with the help of the `Series` command in `Mathematica`. The quantities ξ, ζ and $\{\nu_j\}_{j=1}^{2J_{max}}$ are determined by equating the coefficients of the expansion order by order.

The dependences of ξ and ζ on the physical parameters of the problem — s, κ and ℓ in the case of Reissner-Nordström — are easily obtained from the lowest coefficients of the expansion. Examples of ξ, ζ for the Reissner-Nordström case are given by Eqs. (154)-(156), (160) and (162).

There are two numerical parameters controlling the approximation: J_{max} and k_{max}. The former is the truncation value that approximates A_k —cf. Eq. (68)— whereas the latter fixes all Taylor expansions introduced in section IV.

Once a numerical resolution k_{max} and J_{max} is fixed, we approximate the values $I_{k_{max}+1}, I_{k_{max}}, \ldots, I_{k_{max}-m+1}$ and iterate the Eq. (63) backwards to obtain

$$
I_{k-m} = -\frac{\alpha_k I_{k+1} + \sum_{i=0}^{m-1} \beta_k^{(i)} I_{k-i}}{\beta_k^m}, \quad k = k_{max}, \ldots, 0 .
$$
$$(175)$$

Unfortunately, the existence of several decaying solutions may lead to an unstable backward iteration. Indeed, the decaying solutions actually *grow* as we iterate the recurrence relation backwards to lower values of k. Therefore any numerical error in one decaying solution will excite modes related to another decaying solution. Depending on the power p of the exponential behavior, the numerical error may grow and contaminate the solution.

The phenomena is easily understood with a concrete example. Let us consider the $3-$order recurrence relation with coefficients (153). Here we treat an electromagnetic perturbation for $\kappa = 0.1$. We fix the Laplace parameter to $s = 1+i$, the angular mode $\ell = 3$ and the numerical resolution to $k_{max} = 200$ and $J_{max} = 10$.

The right-hand-side of Eq. (174), calculated at $k = k_{max}$, provides error estimates $\mathcal{E}^{(1)}$ and $\mathcal{E}^{(2)}$ for the approximated asymptotic values of the solutions $I_{k_{max}}^{(1)}$ and $I_{k_{max}}^{(2)}$ — see Eqs. (154)-(156). The error $\mathcal{E}^{(1)}$ excites $I^{(2)}$-modes that behave as v^k ($|v| < 1$). For $k < N_{max}$, the error growth is faster than the behavior of $I_{N_{max}}^{(1)}$ itself. Thus the instability occurs — see the left panel of Fig. 6. On the contrary, the error $\mathcal{E}^{(2)}$ excites $I^{(1)}$-modes behaving merely as $e^{-\xi\sqrt{k}}$, which does not affect the solution $I_k^{(2)}$ — see right panel of Fig. 6.

Figure 6 displays these unstable solutions which we denote here by $\tilde{I}_k^{(\ell)}$. However, we can construct new solutions $I_k^{(\ell)}$ and filter the instability of the raw solutions $\tilde{I}_k^{(\ell)}$ via the linear combination

$$
I_k^{(\ell)} = \sum_{\ell'=\ell}^{m} \varkappa_{\ell'}^\ell \tilde{I}_k^{(\ell')} . \quad (176)
$$

The coefficients of the linear combination (176) are fixed by imposing (72) and (73). Fig. 6 depicts the filtered solution $I_k^{(\ell)}$ constructed via the backward recurrence relation.

[1] S. Chandrasekhar, *The Mathematical Theory of Black Holes* (Oxford University Press, Oxford, England, 1983).

[2] K. D. Kokkotas and B. G. Schmidt, "Quasi-normal modes of stars and black holes," Living Rev. Relativ. **2**, 2 (1999), http://www.livingreviews.org/lrr-1999-2.

[3] H.-P. Nollert, "Quasinormal modes: The characteristic "sound" of black holes and neutron stars," Class. Quantum Grav. **16**, R159 (1999).

[4] Emanuele Berti, Vitor Cardoso, and Andrei O. Starinets, "Quasinormal modes of black holes and black branes," Class.

Quantum Grav. **26**, 163001 (2009), arXiv:0905.2975 [gr-qc].

[5] R. A. Konoplya and A. Zhidenko, "Quasinormal modes of black holes: From astrophysics to string theory," Rev. Mod. Phys. **83**, 793–836 (2011), arXiv:1102.4014 [gr-qc].

[6] R. Price, "Nonspherical perturbations of relativistic gravitational collapse. I. Scalar and gravitational perturtbations," Phys. Rev. D **5**, 2419 (1972).

[7] C. Gundlach, R. Price, and J. Pullin, "Late-time behaviour of stellar collapse and explosions: I. linearized perturbations," Phys. Rev. D **49**, 883 (1994), arXiv:9307009 [gr-qc].
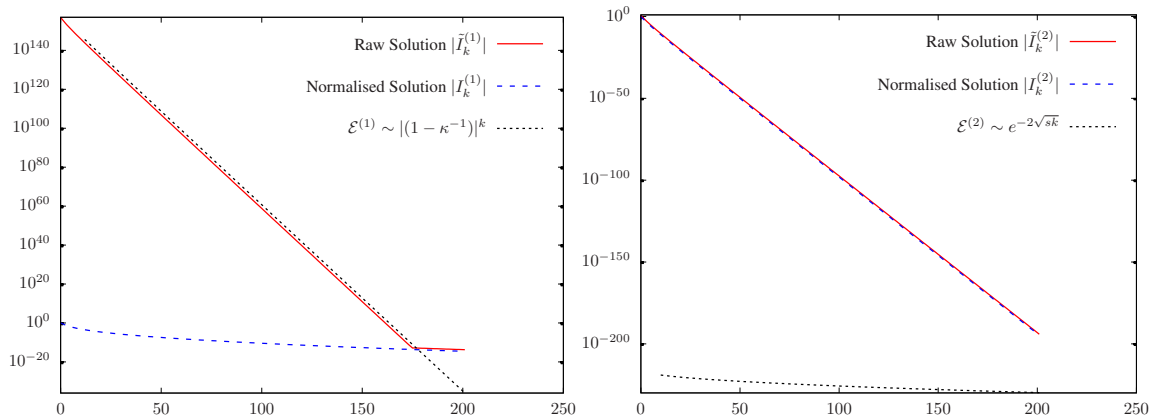
FIG. 6. Unstable behavior from the backward iteration of the recurrence relation (153). The solutions are obtained for an electromagnetic perturbation with parameters $s = 1 + i$, $\kappa = 0.1$, $\ell = 3$ and numerical resolution $N_{\max} = 200$, $J_{\max} = 10$. Left panel: the raw solution $\tilde{I}_k^{(1)} \sim e^{-2\sqrt{sk}}$ (red solid line) is unstable since the numerical error $\mathcal{E}^{(1)}$ (dotted black line) excites $I^{(2)}-$modes growing as $|1 - \kappa^{-1}|^k$ for $k < N_{\max}$. Right panel: the raw solution $\tilde{I}_k^{(2)} \sim |1 - \kappa^{-1}|^k$ (red solid line) is not affected by the numerical error $\mathcal{E}^{(2)} \sim e^{-2\sqrt{sk}}$ (dotted black line). The instability is filtered via the linear combination (176), which normalizes the solution according to (73) (blue dashed line).

[8] Philippe Lalanne, Wei Yan, Kevin Vynck, Christophe Sauvan, and Jean-Paul Hugonin, "Light inter-action with photonic and plasmonic resonances," Laser & Photonics Reviews **12**, 1700113 (2018), https://onlinelibrary.wiley.com/doi/pdf/10.1002/lpor.201700113.

[9] S. Dyatlov and M. Zworski, "Mathematical theory of scattering resonances," (book in preparation; http://math.mit.edu/ dyat-lov/res/).

[10] Maciej Zworski, "Mathematical study of scattering reso-nances," Bulletin of Mathematical Sciences **7**, 1–85 (2017).

[11] Marcus Ansorg and Rodrigo Panosso Macedo, "Spectral de-composition of black-hole perturbations on hyperboloidal slices," Phys. Rev. **D93**, 124016 (2016), arXiv:1604.02261 [gr-qc].

[12] Anil Zenginoglu, "A Geometric framework for black hole per-turbations," Phys. Rev. **D83**, 127502 (2011), arXiv:1102.2451 [gr-qc].

[13] J.L. Friedman and B.F. Schutz, "On the stability of relativistic systems," Astrophys.J. **200**, 204–220 (1975).

[14] B. Schmidt, "On relativistic stellar oscillations," Gravity Re-search Foundation essay (1993).

[15] Martin Ammon, Sebastian Grieninger, Amadeo Jimenez-Alba, Rodrigo P. Macedo, and Luis Melgar, "Holographic quenches and anomalous transport," JHEP **09**, 131 (2016), arXiv:1607.06817 [hep-th].

[16] Hakan Andreasson, "The Einstein-Vlasov system / kinetic the-ory," Living Rev. Rel. **8**, 2 (2005), arXiv:gr-qc/0502091 [gr-qc].

[17] Roberto Emparan and Harvey S. Reall, "Black Holes in Higher Dimensions," Living Rev. Rel. **11**, 6 (2008), arXiv:0801.3471 [hep-th].

[18] G. T. Horowitz, *Black Holes in Higher Dimensions, by Gary T. Horowitz*, (Cambridge Univ. Pr., 2012).

[19] Martin Ammon and Johanna Erdmenger, *Gauge/gravity duality* (Cambridge Univ. Pr., Cambridge, UK, 2015).

[20] Horatiu Nastase, *Introduction to the AdS/CFT Correspondence* (Cambridge Univ. Pr., Cambridge, UK, 2015).

[21] F. M. Paiva, M. J. Reboucas, and Malcolm A. H. Mac-Callum, "On limits of space-times: A Coordinate - free ap-proach," Class. Quant. Grav. **10**, 1165–1178 (1993), arXiv:gr-qc/9302005 [gr-qc].

[22] Robert P. Geroch, "Limits of spacetimes," Commun. Math. Phys. **13**, 180–193 (1969).

[23] S. W. Hawking and G. F. R. Ellis, *The large scale structure of space-time* (Cambridge University Press, 1973).

[24] Sean M. Carroll, Matthew C. Johnson, and Lisa Randall, "Ex-tremal limits and black hole entropy," JHEP **11**, 109 (2009), arXiv:0901.0931 [hep-th].

[25] Ingemar Bengtsson, Soren Holst, and Emma Jakobsson, "Clas-sics Illustrated: Limits of Spacetimes," Class. Quant. Grav. **31**, 205008 (2014), arXiv:1406.4326 [gr-qc].

[26] Hari K. Kunduri and James Lucietti, "Classification of near-horizon geometries of extremal black holes," Living Reviews in Relativity **16**, 8 (2013).

[27] B. Bertotti, "Uniform electromagnetic field in the theory of gen-eral relativity," Phys. Rev. **116**, 1331–1333 (1959).

[28] Robinson I., "A solution of the Maxwell-Einstein equations," Bull. Acad. Polon. Sci. **7**, 351 (1959).

[29] Edward W. Leaver, "Quasinormal modes of Reissner-Nordström black holes," Phys. Rev. D **41**, 2986–2997 (1990).

[30] Anil Zenginoglu, "Hyperboloidal foliations and scri-fixing," Class. Quant. Grav. **25**, 145002 (2008), arXiv:0712.4333 [gr-qc].

[31] Dieter R. Brill, John M. Cavallo, and James A. Isenberg, "K-surfaces in the Schwarzschild space-time and the construction of lattice cosmologies," Journal of Mathematical Physics **21**, 2789–2796 (1980).

[32] Edward Malec and Niall O'Murchadha, "The general spher-ically symmetric constant mean curvature foliations of the Schwarzschild solution," Phys. Rev. **D80**, 024017 (2009), arXiv:0903.4779 [gr-qc].

[33] Patrick Tuite and Niall O Murchadha, "Constant Mean Cur-vature Slices of the Reissner-Nordström Spacetime," (2013), arXiv:1307.4657 [gr-qc].

[34] David Schinkel, Rodrigo Panosso Macedo, and Marcus An-sorg, "Axisymmetric constant mean curvature slices in the Kerr space-time," Class. Quant. Grav. **31**, 075017 (2014), arXiv:1310.4699 [gr-qc].

[35] David Schinkel, Marcus Ansorg, and Rodrigo

Panosso Macedo, "Initial data for perturbed Kerr black holes on hyperboloidal slices," Class. Quant. Grav. **31**, 165001 (2014), arXiv:1301.6984 [gr-qc].

[36] Anil Zenginoglu, "Hyperboloidal layers for hyperbolic equations on unbounded domains," J. Comput. Phys. **230**, 2286–2302 (2011), arXiv:1008.3809 [math.NA].

[37] Peter Hubner, "A Scheme to numerically evolve data for the conformal Einstein equation," Class. Quant. Grav. **16**, 2823–2843 (1999), arXiv:gr-qc/9903088 [gr-qc].

[38] Jörg Frauendiener and Matthias Hein, "Numerical evolution of axisymmetric, isolated systems in general relativity," Phys. Rev. D **66**, 124004 (2002).

[39] James M. Bardeen, Olivier Sarbach, and Luisa T. Buchman, "Tetrad formalism for numerical relativity on conformally compactified constant mean curvature hypersurfaces," Phys. Rev. **D83**, 104045 (2011), arXiv:1101.5479 [gr-qc].

[40] Oliver Rinne, "An Axisymmetric evolution code for the Einstein equations on hyperboloidal slices," Class. Quant. Grav. **27**, 035014 (2010), arXiv:0910.0139 [gr-qc].

[41] Oliver Rinne and Vincent Moncrief, "Hyperboloidal Einstein-matter evolution and tails for scalar and Yang-Mills fields," Class. Quant. Grav. **30**, 095009 (2013), arXiv:1301.6174 [gr-qc].

[42] Alex Vañó-Viñuales, Sascha Husa, and David Hilditch, "Spherical symmetry as a test case for unconstrained hyperboloidal evolution," Class. Quant. Grav. **32**, 175010 (2015), arXiv:1412.3827 [gr-qc].

[43] Manuel D. Morales and Olivier Sarbach, "Evolution of scalar fields surrounding black holes on compactified constant mean curvature hypersurfaces," Phys. Rev. **D95**, 044001 (2017), arXiv:1609.05756 [gr-qc].

[44] David Hilditch, Enno Harms, Marcus Bugner, Hannes Rüter, and Bernd Brügmann, "The evolution of hyperboloidal data with the dual foliation formalism: Mathematical analysis and wave equation tests," Class. Quant. Grav. **35**, 055003 (2018), arXiv:1609.08949 [gr-qc].

[45] Alex Vañó-Viñuales and Sascha Husa, "Spherical symmetry as a test case for unconstrained hyperboloidal evolution II: gauge conditions," Class. Quant. Grav. **35**, 045014 (2018), arXiv:1705.06298 [gr-qc].

[46] Rodrigo Panosso Macedo and Marcus Ansorg, "Axisymmetric fully spectral code for hyperbolic equations," J. Comput. Phys. **276**, 357–379 (2014), arXiv:1402.7343 [physics.comp-ph].

[47] Anil Zenginoglu, Dario Nunez, and Sascha Husa, "Gravitational perturbations of Schwarzschild spacetime at null infinity and the hyperboloidal initial value problem," Class. Quant. Grav. **26**, 035009 (2009), arXiv:0810.1929 [gr-qc].

[48] Anil Zenginoglu, "Asymptotics of black hole perturbations," Class. Quant. Grav. **27**, 045015 (2010), arXiv:0911.2450 [gr-qc].

[49] Istvan Racz and Gabor Zsolt Toth, "Numerical investigation of the late-time Kerr tails," Class. Quant. Grav. **28**, 195003 (2011), arXiv:1104.4199 [gr-qc].

[50] Michael Jasiulek, "Hyperboloidal slices for the wave equation of Kerr-Schild metrics and numerical applications," Class. Quant. Grav. **29**, 015008 (2012), arXiv:1109.2513 [gr-qc].

[51] Enno Harms, Sebastiano Bernuzzi, and Bernd Brügmann, "Numerical solution of the 2+1 Teukolsky equation on a hyperboloidal and horizon penetrating foliation of Kerr and application to late-time decays," Class. Quant. Grav. **30**, 115013 (2013), arXiv:1301.1591 [gr-qc].

[52] Robert M. Wald, *General relativity* (The University of Chicago Press, Chicago, 1984).

[53] E.W. Leaver, "An analytic representation for the quasi-normal modes of Kerr black holes," Proc. R. Soc. London, Ser. A **402**, 285–298 (1985).

[54] E. W. Leaver, "Spectral decomposition of the perturbation response of the Schwarzschild geometry," Phys. Rev. D **34**, 384–408 (1986).

[55] A. Bachelot and A. Motet-Bachelot, "Les résonances d'un trou noir de Schwarzschild." Ann. Inst. Henri Poincaré, Phys. Théor., Vol. 59, No. 1, p. 3 - 68 **59**, 3–68 (1993).

[56] D. Batic, M. Nowakowski, and K. Redway, "Some exact quasinormal frequencies of a massless scalar field in Schwarzschild spacetime," Phys. Rev. **D98**, 024017 (2018), arXiv:1807.04513 [gr-qc].

[57] Rodrigo Panosso Macedo, "No exact quasinormal frequencies of a massless scalar field in Schwarzschild spacetime," (2018), arXiv:1807.05940 [gr-qc].

[58] Rodrigo Panosso Macedo, "Late time decay of higher-dimensional black holes along future null infinity," (In preparation).

[59] Vincent Moncrief, "Odd-parity stability of a Reissner-Nordström black hole," Phys. Rev. D **9**, 2707–2709 (1974).

[60] Vincent Moncrief, "Stability of Reissner-Nordström black holes," Phys. Rev. D **10**, 1057–1059 (1974).

[61] Vincent Moncrief, "Gauge-invariant perturbations of Reissner-Nordström black holes," Phys. Rev. D **12**, 1526–1537 (1975).

[62] Frank J. Zerilli, "Perturbation analysis for gravitational and electromagnetic radiation in a Reissner-Nordström geometry," Phys. Rev. D **9**, 860–868 (1974).

[63] Hisashi Onozawa, Takashi Mishima, Takashi Okamura, and Hideki Ishihara, "Quasinormal modes of maximally charged black holes," Phys. Rev. **D53**, 7033–7040 (1996), arXiv:gr-qc/9603021 [gr-qc].

[64] Juan A. Valiente Kroon, *Conformal Methods in General Relativity* (Cambridge University Press, Cambridge, 2016).

[65] Maurício Richartz, "Quasinormal modes of extremal black holes," Phys. Rev. **D93**, 064062 (2016), arXiv:1509.04260 [gr-qc].

[66] Jose Luis Jaramillo, Rodrigo Panosso Macedo, Philipp Moesta, and Luciano Rezzolla, "Black-hole horizons as probes of black-hole dynamics I: post-merger recoil in head-on collisions," Phys. Rev. **D85**, 084030 (2012), arXiv:1108.0060 [gr-qc].

[67] Jose Luis Jaramillo, Rodrigo P. Macedo, Philipp Moesta, and Luciano Rezzolla, "Black-hole horizons as probes of black-hole dynamics II: geometrical insights," Phys. Rev. **D85**, 084031 (2012), arXiv:1108.0061 [gr-qc].

[68] J. L. Jaramillo, R. P. Macedo, P. Moesta, and L. Rezzolla, "Towards a cross-correlation approach to strong-field dynamics in Black Hole spacetimes," *Proceedings, Spanish Relativity Meeting : Towards new paradigms. (ERE 2011): Madrid, Spain, August 29-September 2, 2011*, AIP Conf. Proc. **1458**, 158–173 (2011), arXiv:1205.3902 [gr-qc].

[69] Anshu Gupta, Badri Krishnan, Alex Nielsen, and Erik Schnetter, "Dynamics of marginally trapped surfaces in a binary black hole merger: Growth and approach to equilibrium," Phys. Rev. **D97**, 084028 (2018), arXiv:1801.07048 [gr-qc].

[70] Ermis Mitsou, "Gravitational radiation from radial infall of a particle into a Schwarzschild black hole. A numerical study of the spectra, quasi-normal modes and power-law tails," Phys. Rev. **D83**, 044039 (2011), arXiv:1012.2028 [gr-qc].

[71] Sebastiano Bernuzzi, Alessandro Nagar, and Anil Zenginoglu, "Binary black hole coalescence in the extreme-mass-ratio limit: testing and improving the effective-one-body multipolar waveform," Phys. Rev. **D83**, 064010 (2011), arXiv:1012.2456 [gr-qc].

[72] Anil Zenginoglu and Gaurav Khanna, "Null infinity waveforms

from extreme-mass-ratio inspirals in Kerr spacetime," Phys. Rev. **X1**, 021017 (2011), arXiv:1108.1816 [gr-qc].

[73] Sebastiano Bernuzzi, Alessandro Nagar, and Anil Zenginoglu, "Binary black hole coalescence in the large-mass-ratio limit: the hyperboloidal layer method and waveforms at null infinity," Phys. Rev. **D84**, 084026 (2011), arXiv:1107.5402 [gr-qc].

[74] Enno Harms, Sebastiano Bernuzzi, Alessandro Nagar, and An Zenginoglu, "A new gravitational wave generation algorithm for particle perturbations of the Kerr spacetime," Class. Quant. Grav. **31**, 245004 (2014), arXiv:1406.5983 [gr-qc].

[75] Enno Harms, Georgios Lukes-Gerakopoulos, Sebastiano Bernuzzi, and Alessandro Nagar, "Asymptotic gravitational wave fluxes from a spinning particle in circular equatorial orbits around a rotating black hole," Phys. Rev. **D93**, 044015 (2016), arXiv:1510.05548 [gr-qc].

[76] Jonathan Thornburg and Barry Wardell, "Scalar self-force for highly eccentric equatorial orbits in Kerr spacetime," Phys. Rev. **D95**, 084043 (2017), arXiv:1610.09319 [gr-qc].

[77] Vitor Cardoso, Shijun Yoshida, Oscar J. C. Dias, and Jose P. S. Lemos, "Late time tails of wave propagation in higher dimensional space-times," Phys. Rev. **D68**, 061503 (2003), arXiv:hep-th/0307122 [hep-th].

[78] Vitor Cardoso and Paolo Pani, "The observational evidence for horizons: from echoes to precision gravitational-wave physics," Nature Astronomy **1**, 586–591 (2003), arXiv:1707.03021 [gr-qc].

[79] J. Sjöstrand, "Non-self-adjoint differential operators, spectral asymptotics and random perturbations," (to appear in *Pseudod-ifferential Operators, Theory and Applications*, Birkhäuser).

[80] E. S. C. Ching, P. T. Leung, A. Maassen van den Brink, W. M. Suen, S. S. Tong, and K. Young, "Quasinormal-mode expansion for waves in open systems," Rev. Mod. Phys. **70**, 1545–1554 (1998).

[81] Horst R. Beyer, "On the completeness of the quasinormal modes of the P"oschl-Teller potential," Commun. Math. Phys. **204**, 397–423 (1999), arXiv:gr-qc/9803034 [gr-qc].

[82] P. D. Lax and R. S Phillips, *Scattering theory*, second edition ed., Pure and Applied Mathematics, Vol. 26 (Academic Press, Boston, 1989).

[83] B. R. Vainberg, "Exterior elliptic problems that depend polynomially on the spectral parameter, and the asymptotic behavior for large values of the time of the solutions of nonstationary problems," Mat. Sb. (N.S.) **92**, 224–241 (1973), translated in Math. USSR-Sb. 21 (1973), 221–239.